VECTOR-BORNE DISEASES

Progress in imaging methods: insights gained into *Plasmodium* biology

Mariana De Niz[1,2], Paul-Christian Burda[1], Gesine Kaiser[1], Hernando A. del Portillo[3,4], Tobias Spielmann[5], Freddy Frischknecht[6]* and Volker T. Heussler[1]**

Abstract | Over the past decade, major advances in imaging techniques have enhanced our understanding of *Plasmodium* spp. parasites and their interplay with mammalian hosts and mosquito vectors. Cryoelectron tomography, cryo-X-ray tomography and super-resolution microscopy have shifted paradigms of sporozoite and gametocyte structure, the process of erythrocyte invasion by merozoites, and the architecture of Maurer's clefts. Intravital time-lapse imaging has been revolutionary for our understanding of pre-erythrocytic stages of rodent *Plasmodium* parasites. Furthermore, high-speed imaging has revealed the link between sporozoite structure and motility, and improvements in time-lapse microscopy have enabled imaging of the entire *Plasmodium falciparum* erythrocytic cycle and the complete *Plasmodium berghei* pre-erythrocytic stages for the first time. In this Review, we discuss the contribution of key imaging tools to these and other discoveries in the malaria field over the past 10 years.

Sporozoite
A motile, crescent-shaped stage of *Plasmodium* spp. parasites; sporozoites are injected into a mammalian host by a mosquito vector.

Gametocytes
Sexual stages of *Plasmodium* spp. parasites. Gametocytes are either male or female gamete precursors and are solely responsible for transmission of the parasite from the vertebrate host to the mosquito.

*These authors contributed equally to this work.

Correspondence to M.D.N and V.T.H.
Institute of Cell Biology, University of Bern, Baltzerstrasse 4, 3012 Bern, Switzerland.
mariana.deniz@glasgow.ac.uk; heussler@izb.unibe.ch

doi:10.1038/nrmicro.2016.158
Published online 28 Nov 2016

Malaria, which is caused by *Plasmodium* spp. parasites, is a major infectious disease that affects the developing world, and there are global efforts that are devoted to generating strategies for its control[1]. Malaria parasites are transmitted through the bite of an infected female *Anopheles* spp. mosquito. Within the vertebrate host, the parasite undergoes two consecutive stages of schizogonic asexual replication (BOX 1). The first stage is clinically silent and takes place in the liver (BOX 1; see the figure, steps 2–8). The second stage occurs following parasite release from the liver into the bloodstream (BOX 1; see the figure, steps 9–14) and is responsible for the clinical manifestation of the disease.

The biology of *Plasmodium* spp. parasites, as well as their interactions with human and mosquito hosts, has been a focus of research for more than a century, and microscopy has historically greatly accelerated progress in this field. In the past decade, revolutionary advances in light and electron microscopy have provided invaluable information about parasite biology and host–pathogen interactions (TABLE 1).

The imaging of parasite architecture in most stages of the life cycle was mainly advanced by various electron microscopy methods, including cryoelectron tomography and cryo-X-ray tomography, as well as by super-resolution fluorescence imaging[2–7]. Techniques such as spinning-disc microscopy, among others, have been pivotal for the elucidation of sporozoite motility[8–10]. Finally, major breakthroughs in time-lapse microscopy enabled the imaging of *Plasmodium* spp. parasites during the complete blood[11] and liver[12] stages of their life cycles *in vitro*. In this Review, we focus on imaging methods that have advanced our understanding of parasite cell biology and host–pathogen interactions in the mammalian host, and have led to important paradigm shifts in our knowledge of malaria during the past decade.

Transmission and the 'skin phase'

During a blood meal, a *Plasmodium*-infected mosquito injects sporozoites into a human host (BOX 1; see the figure, step 1; Supplementary information S1 (movie)). In turn, human-to-vector transmission occurs when, during blood feeding, a mosquito ingests gametocytes that are circulating in the blood of an infected host (BOX 1; see the figure, step 15).

Sporozoite architecture. Mature sporozoites (FIG. 1a) are slender cells that form in oocysts at the mosquito midgut wall. They are approximately 10 µm long, just less than 1 µm thick and are slightly curved[13]. 3D cryoelectron tomography has increased our understanding of the relevance of sporozoite architecture, in particular with regard to sporozoite migration. This technique enables the examination of native and hydrated structural features, as well as the study of different functional states of molecules within the sample (TABLE 1). Four key observations in terms of sporozoite architecture are discussed below.

Many studies that used classic electron microscopy methods showed the overall architecture of sporozoites and similar parasite forms. For example, it was found

Author addresses

[1]*Institute of Cell Biology, University of Bern, Baltzerstrasse 4, 3012 Bern, Switzerland.*
[2]*Present addresses: Department of Immunology and Infectious Diseases, Harvard T.H. Chan School of Public Health, 677 Huntington Avenue, Boston, Massachusetts 02115, USA, and Wellcome Trust Centre for Molecular Parasitology, University of Glasgow, 120 University Place, Glasgow, G12 8TA, UK.*
[3]*Catalan Institution for Research and Advanced Studies (ICREA) at Barcelona Institute for Global Health (ISGlobal), Barcelona Centre for International Health Research (CRESIB), Hospital Clínic-Universitat de Barcelona, 08036 Barcelona, Spain.*
[4]*ICREA at Institut d'Investigació Germans Trias i Pujol (IGTP), Can Ruti Campus, 08916 Badalona, Barcelona, Spain.*
[5]*Bernhard Nocht Institute for Tropical Medicine, Bernhard-Nocht-Strasse 74, D-20359 Hamburg, Germany.*
[6]*Parasitology, Center for Infectious Diseases, Heidelberg University School of Medicine, Im Neuenheimer Feld 324, 69120 Heidelberg, Germany.*

that the polar ring at the apical end could function as a microtubule-organizing centre[14]. The so-called subpellicular microtubules are arranged as a 'cage' that encases secretory organelles (FIG. 1b). In sporozoites, unlike in most other parasite forms, most microtubules cover two-thirds of the circumference of the cage, whereas a single microtubule is found in the remaining one-third[13]. Cryoelectron tomography revealed that the apical polar ring is tilted away from the single microtubule, seemingly being pushed towards the external substrate[3]. Similar to the invasive forms of other apicomplexan parasites, sporozoites release the contents of their secretory vesicles through the apical polar ring[15]. Therefore, the tilt of this polar ring might direct the secretion of proteins that are important for adhesion directly onto the substrate.

The second insight into sporozoite architecture came from findings in *Plasmodium berghei* that revealed the existence of a thickened subpellicular network (SPN) in sporozoites from the mosquito salivary gland but not in sporozoites that were directly isolated from the oocysts in the mosquito midgut[3,16] (FIG. 1c). In salivary gland sporozoites, the SPN protein inner membrane complex 1 (IMC1) was shown to have relocated from the cytoplasm, where it is found in midgut sporozoites, to the SPN[17], which suggests that the SPN builds up during sporozoite maturation. Salivary gland sporozoites, but not midgut sporozoites, are crescent shaped and capable of gliding motility. These findings suggest that the crescent shape results from the assembly of the SPN. The crescent shape of mature sporozoites might have evolved to lower the energy costs of migrating through tissues or as a result of preferred binding to blood vessels, which have the same curvature as sporozoites[18,19].

Two further structural findings that were revealed by 3D cryoelectron tomography of *P. berghei* sporozoites are the enigmatic presence of filopodium-like extensions of the plasma membrane at the front of some sporozoites[16] (FIG. 1d), and the discovery of an unknown protein inside the lumen of the subpellicular microtubules (FIG. 1c) that possibly has a role in stabilizing these microtubules[2].

Although 3D cryoelectron tomography has indeed provided key details about sporozoite architecture, it relies on static imaging, which makes it impossible to directly assess the functional relevance of these architectural characteristics. However, the combination of static and dynamic microscopy methods both *in vivo* and *in vitro* has become a powerful tool for elucidating the link between structure and function.

Sporozoite migration and the skin phase. Wide-field, confocal or spinning-disk intravital microscopy (IVM)[8,19–24] were used to visualize mosquito-to-vertebrate transmission of *P. berghei* parasites *in vivo* (BOX 1; see the figure, step 1; BOX 2; see the figure, part **b**). These studies (reviewed in detail in REFS 25,26) revealed that sporozoites are deposited in the dermis and immediately start migrating at speeds of 1–2 μm s^{-1} (REF. 20). Sporozoite movement follows random paths in the ear but more linear paths in the dermis of the mouse tail[22]. Interestingly, *P. berghei* sporozoites were shown to migrate in structured microenvironments *in vitro*, in which they show similar linear or random paths, depending on the environment. This suggests that their motility *in vivo* is dictated by characteristics of their local environment, such as the presence of collagen fibres[22]. Sporozoites also transmigrate through cells aided by the secretion of pore-forming proteins[23,24]. They can enter either blood capillaries or lymph vessels, or they can remain in the skin[8,27]. A long-standing misconception in the malaria field was that sporozoites are injected directly into blood vessels by the mosquito proboscis. IVM that was carried out on *P. berghei*-infected mice, together with experiments that removed the bite site and interrupted mosquito feeding, proved that this was not the case. Instead, sporozoites are injected into the connective tissue of the skin[28]. These findings suggest that the skin phase of *Plasmodium* spp. infection is the first possible target for prophylaxis[29,30].

To actively migrate, sporozoites need to attach to a substrate. Total internal reflection fluorescence microscopy (TIRFM) is a powerful method to visualize single-molecule fluorescence at the immediate interface of substrate and cell. Similarly, reflection interference contrast microscopy (RICM) enables the measurement of inter-surface distances with nanometric precision and millisecond time resolution to study adhesion dynamics. Both techniques showed that *P. berghei* sporozoites attach to a flat substrate in a stepwise manner[10,31]. Using RICM, it was also shown that when the sporozoite is motile, the distinct adhesion sites detach and re-attach rapidly in a manner that is dependent on actin dynamics and the surface protein thrombospondin-related anonymous protein (TRAP)[10]. This suggests that rapid adhesion turnover is crucial for the sporozoite to obtain high speed (FIG. 1e).

The forces that are exerted by the sporozoites onto the substrate to enable movement are small in comparison to those exerted by much larger mammalian cells, such as fibroblasts[10]. Nevertheless, using a sensitive traction force microscopy method, a study was able to distinguish zones of different force transduction during *P. berghei* sporozoite motility[10]. Force generation was also shown to depend on the presence of dynamic actin filaments. To investigate the role of surface proteins, another investigation used nanopatterned substrates that enable sporozoites to attach

Oocysts
Cysts that develop from parasite ookinetes on the outside of the mosquito midgut, under the basal lamina, and in which asexual replication produces hundreds of sporozoites.

Secretory vesicles
Membrane-bound vesicles that are derived from intracellular organelles and contain material for transport beyond the plasma membrane.

Subpellicular network
(SPN). A skeletal component of organisms such as *Plasmodium* spp., consisting of a network of intermediate filaments on the cytoplasmic side of the inner membrane complex (IMC).

Pore-forming proteins
Secreted, monomeric, water-soluble proteins that, in proximity to membranes, oligomerize into ring-like structures to enable membrane insertion and pore formation.

Actin
A highly abundant structural protein that exists in a monomeric globular form (G-actin) and can polymerize into microfilaments (F-actin) to form the actin cytoskeleton, which supports cellular shape and cell migration, and provides tracks for the transport of vesicles and organelles within the cell.

Basal lamina
A layer of extracellular matrix that is secreted by epithelial cells and on which the epithelium lies.

only to 10 nm-wide gold particles that are spread at large distances from each other[32]. Remarkably, sporozoites were still moving on substrates for which only about 100 molecules could have attached the parasite to the substrate. One of these molecules, TRAP, is essential for sporozoite gliding motility[33]: sporozoites and other motile apicomplexan stages move forwards when TRAP family adhesins bind to the substrate. Sporozoites need to be activated to undergo gliding. This activation has been investigated using a fluorescence resonance energy transfer (FRET)-based calcium sensor[34] and a fluorescently tagged actin-binding protein[35], showing that an increased calcium concentration leads to the secretion of TRAP followed by the organization of actin filaments and, hence, motility. The speed of parasite forward movement was presumed to equal the speed of the retrograde movement of the adhesins along the parasite surface[36]. However, subsequent studies have used laser traps to identify a distinct function for different members of the TRAP family of membrane proteins[37–39]. To this end, either *P. berghei* sporozoites were trapped and directly probed[37] or small beads

Box 1 | The *Plasmodium* spp. life cycle

Malaria is a vector-borne disease that is caused by *Plasmodium* spp. parasites, which are transmitted by female *Anopheles* spp. mosquitoes[1]. During a blood meal, the mosquito injects a small number of *Plasmodium* spp. sporozoites into the skin (see the figure, step 1). Some parasites remain in the skin and are eliminated by resident macrophages. Others migrate to the lymph nodes, where they are also eliminated, whereas some reach the bloodstream and are transported passively to the liver[25,44]. Following entry into the liver vasculature, sporozoites glide along the sinusoids (step 2) and transmigrate through either Kupffer cells or endothelial cells to reach hepatocytes[9] (step 3). Sporozoites transmigrate through several hepatocytes before invading one[136] (step 4). In the invaded hepatocyte, they reside in a parasitophorous vacuole (PV; step 5) and will undergo enormous asexual replication (steps 6–7) without eliciting clinical symptoms in the host. Some *Plasmodium* spp. can remain dormant in the liver for extended periods of time, causing relapses at a later time. In most species, liver-stage completion is marked by the release of thousands of merozoites into the peripheral circulation within merosomes (step 8), which are transported to the small capillaries of the lungs, where they rupture and release the merozoites[45–47]. Each merozoite is capable of invading a red blood cell (RBC), marking the beginning of the erythrocytic stages of infection (step 9). The pre-patency (the period until parasites appear in the blood) ranges from 3–30 days, depending on the parasite species as well as several other factors, such as previous host immune status, previous host exposure to parasites and the number of sporozoites inoculated. Following the invasion of RBCs, the parasites develop into ring stages (step 10), then into trophozoites (step 11) and finally into schizonts (step 12), which rupture and release up to 36 merozoites into the bloodstream (step 13). Asexual replication in the form of multiple cycles of schizogony exponentially increases the parasite burden with each cycle[11] (steps 9–13). To avoid clearance by the spleen, trophozoites and schizonts of *Plasmodium falciparum* sequester in the vasculature, leading to the pathology and severity associated with this malaria parasite. Exponential asexual replication also results in the generation of sexual stages (step 14), which can be transmitted to a susceptible mosquito during a blood meal[97,100] (step 15). Following transmission to the vector, male and female gametocytes develop into male and female gametes, which are liberated and will fuse inside the midgut (step 16), giving rise to motile zygotes, or ookinetes (step 17), which leave the lumen of the midgut and settle under the basal lamina (step 18). There, they develop into oocysts, in which hundreds of sporozoites are produced (step 19). Finally, the oocysts burst, and the released sporozoites are transported through the haemolymph (step 20), eventually reaching and invading the salivary glands of the mosquito (step 21), from which they can again be injected into a new host during a mosquito bite (step 1). The complete cycle takes several weeks (see the figure, lower panel; the *x* axis shows the timing of each event, beginning with the bite of an infected mosquito on day 0, and the duration of each stage, whereas the *y* axis shows the approximate parasite numbers at each stage).

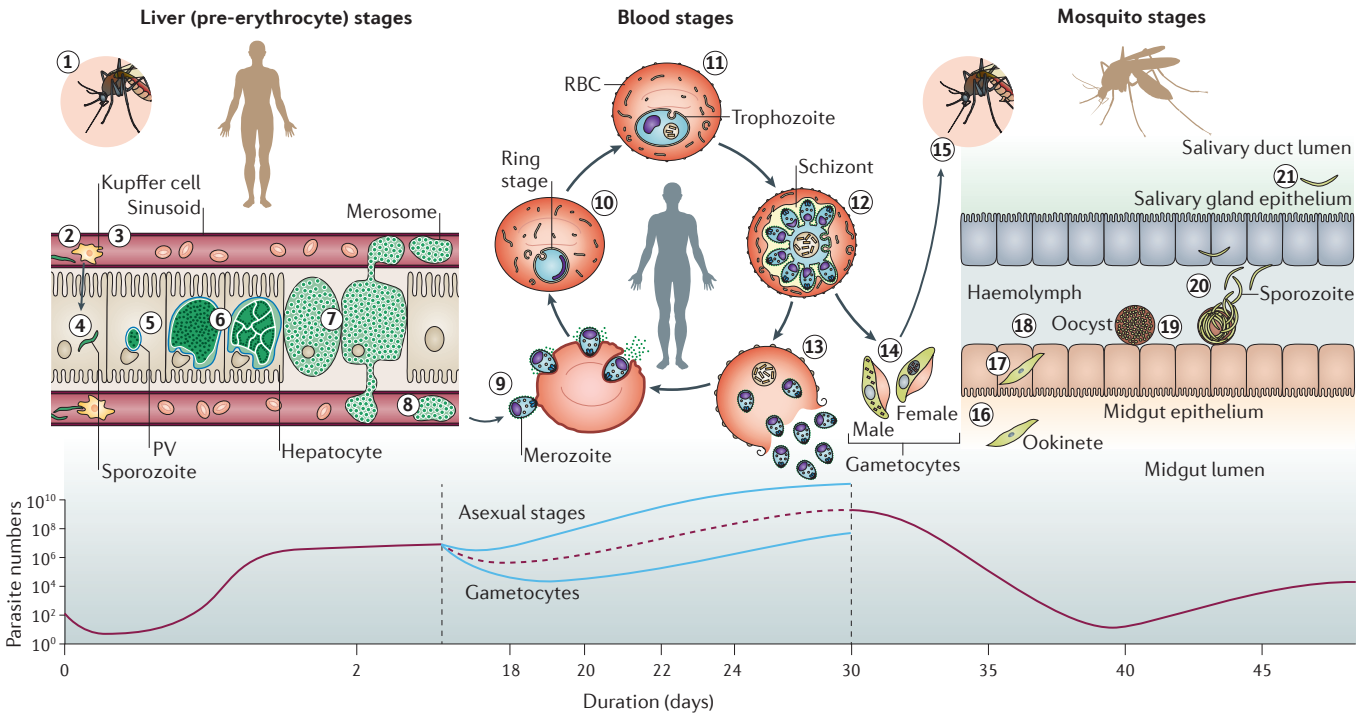

Table 1 | **Advanced imaging techniques used to study *Plasmodium* spp. parasites**

Imaging classification	Principle	Applications in *Plasmodium* spp.	Advantages	Limitations
Atomic-force microscopy and spectroscopy	• Measurement of surface topography and receptor–ligand interaction forces at a very high resolution[128]	• Identification of knobs[121–124] • Measurement of CD36–PfEMP1 binding forces[120] • Topography of infected hepatocytes[140] • Investigation of spectrin network during infection[99]	• Near-atomic resolution • Versatility of applications: can be used for defining chemical, biological and physical properties of individual cells and molecules	• Extensive training required • Live cell imaging required for research involving receptor–ligand interactions or surface topology of infected RBCs • Specialized tips and functionalization, as well as exhaustive optimization required
Cryoelectron tomography	• Detailed imaging of cellular structures at the molecular level[141,142] • Samples are immobilized in vitreous ice and visualized under cryogenic conditions	• Investigation of the structure and architecture of sporozoites[2–4,16,138], merozoites[143], infected RBCs[4,144] and gametocytes[98]	• Nanometre resolution • Preservation of biological structures • No artefacts from fixation or embedding • Can be combined with fluorescence microscopy	• Limited sample thickness for 3D imaging • Specialized equipment necessary • Extensive training required • High cost
Cryo-X-ray tomography	• Imaging of specimens up to 10 µm thick using soft X-rays[145], which are strongly absorbed by carbon-rich structures in a spectral window termed the 'water window'	• Imaging of *P. falciparum*–merozoite attachment and invasion[74] • Study of haemozoin and Maurer's clefts[105] • Imaging of gametocyte morphology[107]	• Nanoscale resolution • Imaging of cryo-preserved, unstained whole cells thicker than 1 µm (near-native-state imaging)	• Specialized equipment necessary • Extensive training required • High cost
Super-resolution fluorescence microscopy	• Nanoscopic resolution of live and fixed fluorescent samples[92,146–148] • Variants include SIM, STED, PALM, STORM and RESOLFT	• Study of LC3B–PVM colocalization (STED)[12] • Study of receptor–ligand partners on RBC invasion (SIM)[7] • Study of RBC and gametocyte architecture (SIM)[106,149]	• No need for extensive embedding and sectioning • Fluorescence allows immediate identification of structures of interest	• Special fluorophores might be required • Some methods are not compatible with RBCs or even with living samples
Confocal and two-photon microscopy	• High resolution of live and fixed fluorescent samples • Diffraction limited • Examples include spinning-disc microscopy[150], two-photon microscopy[151,152] and harmonic generation microscopy[153,154], and single-point and scanning confocal microscopy[155]	• Imaging of sporozoites[8,9,24] • Imaging of infected RBCs and hepatocytes[11,12] • Identification of multiple parasite organelles and host–pathogen interactions[5,45,47,53,60,156]	• Better resolution and penetration depth than epifluorescence microscopy • Production of thin optical sections possible • Multidimensional imaging possible • Compatible with living cells and animals • High-speed imaging possible (spinning-disc microscopy)	• Limited by the number of excitation wavelengths available with lasers • High-intensity lasers can damage living samples • High cost (two-photon excitation microscopy)
Photobleaching and photoconversion-based techniques	• Characterization of the kinetic properties of proteins in living cells or animals, and quantification and modelling of these parameters • Modalities include FRAP, iFRAP, FLAP and FLIP	• Study of protein export in infected RBCs[11,157] • Study of organelle continuity in liver-stage parasites, liver-stage host–pathogen interactions and the liver-stage PVM[52] • Study of sporozoite proteins involved in motility[3,35,156]	• Compatible with living samples • Easy measurement of lateral diffusion • High sensitivity	• High-energy laser can induce phototoxicity in living samples • Limited use if fluorescence intensity of protein is low

Table 1 (cont.) | **Advanced imaging techniques used to study *Plasmodium* spp. parasites**

Imaging classification	Principle	Applications in *Plasmodium* spp.	Advantages	Limitations
Surface-sensitive techniques	• Measurement of forces and dynamic interactions between cells and the surface or in cell–cell interactions • Modalities include optical and/or magnetic tweezers[39,158], RICM and TIRFM	• Investigation of sporozoite–substrate adhesion[10,31,37,38] • Investigation of merozoite invasion[93]	• Easy to build (TIRFM and RICM equipment) • Does not require specific labelling with fluorophores (RICM) • High resolution • High sensitivity (TIRFM) • Can be combined with different illumination modes	• Provides no information on biochemical specificities of contact regions (RICM) • Imaging confined to a limited space marking the interface between two surfaces
Intravital microscopy	• Imaging of processes in living animals through exposure of an organ through coverslips or imaging windows • Modalities include confocal, spinning-disc and two-photon microscopy[159,160]	• Imaging of sporozoites in the mouse skin and liver[8,9,46] • Imaging of developing liver stages[12,45] • Imaging of host–pathogen interactions[8,12,19,45] • Imaging of infected RBCs in the brain[137], placenta[161], lymph nodes[8,162,163], spleen[164,165] and adipose tissue[165]	• Imaging of events *in vivo* in a multi-system organism rather than isolated cells • High resolution • Medium penetration depth	• Some forms of this procedure are end-point • Expertise in surgery and animal handling required

FLAP, fluorescence localization after photobleaching; FLIP, fluorescence loss in photobleaching; FRAP, fluorescence recovery after photobleaching; iFRAP, inverse fluorescence recovery after photobleaching; LC3B, microtubule-associated protein 1 light chain 3B; PALM, photoactivated localization microscopy; *P. falciparum*, *Plasmodium falciparum*; PfEMP1, erythrocyte membrane protein 1; PVM, parasitophorous vacuole membrane; RBC, red blood cell; RESOLFT, reversible saturable optical linear fluorescence transitions; RICM, reflection interference contrast microscopy; SIM, structured illumination microscopy; STED, stimulated emission depletion; STORM, stochastic optical reconstruction microscopy; TIRFM, total internal reflection fluorescence microscopy.

were trapped and brought into contact with the sporozoites[38]. These biophysical studies showed that force production for motility is not linearly coupled to the retrograde flow of the adhesins but requires complex macromolecular interactions. These assays, coupled to high-speed image acquisition, revealed different types of interaction between the TRAP-family adhesins and the actin cytoskeleton, and suggested that they act together to form macromolecular assemblies that are important for applying force. Importantly, these findings imply that sporozoites have evolved to apply force mainly for adhesion and not for the retrograde flow of the adhesins. The detailed interactions between adhesins and the force-producing motor are not known to date.

IVM also revealed that some *P. berghei* sporozoites injected into mice can successfully develop in cells of the dermis, epidermis and hair follicles[27,40]. Most strikingly, skin merozoites and the detachment of merosomes[27] were observed, possibly a relic of the shared ancestry of these mammalian malaria parasites with their avian counterparts, which develop within the skin (although in different cell types)[41]. Interestingly, a small proportion of parasites were able to persist for weeks in association with hair follicles[27], which are considered an immune-privileged site. Additional investigation is required to determine whether this constitutes a new niche or source for recurrent malaria infections. Moreover, IVM also showed that 10–20% of transmitted sporozoites accumulate in the draining lymph nodes, where they can induce immune responses[8,42]. Whether or how these alter an ongoing infection remains to be shown, and further studies are required to investigate sporozoite-induced immune reactions in the lymph nodes.

The liver stages

Within hepatocytes, *Plasmodium* spp. parasites undergo a clinically silent phase of exponential replication (BOX 1; see the figure, steps 2–4; Supplementary information S2 (movie)). As well as merozoite numbers, the duration of the liver stage of infection differs substantially across host and parasite species: this stage typically lasts 2–3 days in rodents and 7–10 days in humans, but some parasite species, such as *Plasmodium vivax* and *Plasmodium ovale*, are able to produce dormant stages that lead to relapses as long as several years after the primary infection.

Sporozoite entry into the liver. Sporozoites arrest in the liver probably owing to both a slower circulation speed in liver sinusoids (BOX 1; see the figure, step 2) and molecular interactions of the parasitic protein circumsporozoite protein (CSP) with highly sulfated proteoglycans (HSPGs) that are presented by hepatocytes through the fenestrae of endothelial cells[43,44]. IVM of exposed liver lobes in combination with genetically modified fluorescent parasites revealed, for the first time, the dynamics of the aggressive cell traversal behaviour of the sporozoite in the living host (BOX 1; see the figure, steps 3–4; BOX 2; see the figure, part **b**; Supplementary information S3 (movie)). Different IVM modalities have been used, including spinning-disc microscopy[45] and high-speed two-photon microscopy, to increase the penetration depth to about 500 µm. Improvements in microscope optical design and the camera technologies that are used for spinning-disc microscopy have enabled the visualization of dynamic events involving the parasite en route to, and within, the liver, in the range of milliseconds.

Merozoites
Daughter parasites that originate from the asexual replication of certain apicomplexan parasites in infected red blood cells or hepatocytes. Merozoites can invade and infect red blood cells.

Merosomes
Hepatocyte-derived membrane vesicles that contain a few to thousands of infectious merozoites that are extruded into the blood circulation.

Sinusoids
Low-pressure, discontinuous blood vessels with a high rate of metabolite and nutrient exchange. Permeability in the sinusoids is enhanced by intercellular clefts and fewer tight junctions in the underlying endothelium.

Circumsporozoite protein
(CSP). The most abundant surface protein of *Plasmodium* spp. sporozoites. CSP is involved in initial hepatocyte binding and invasion.

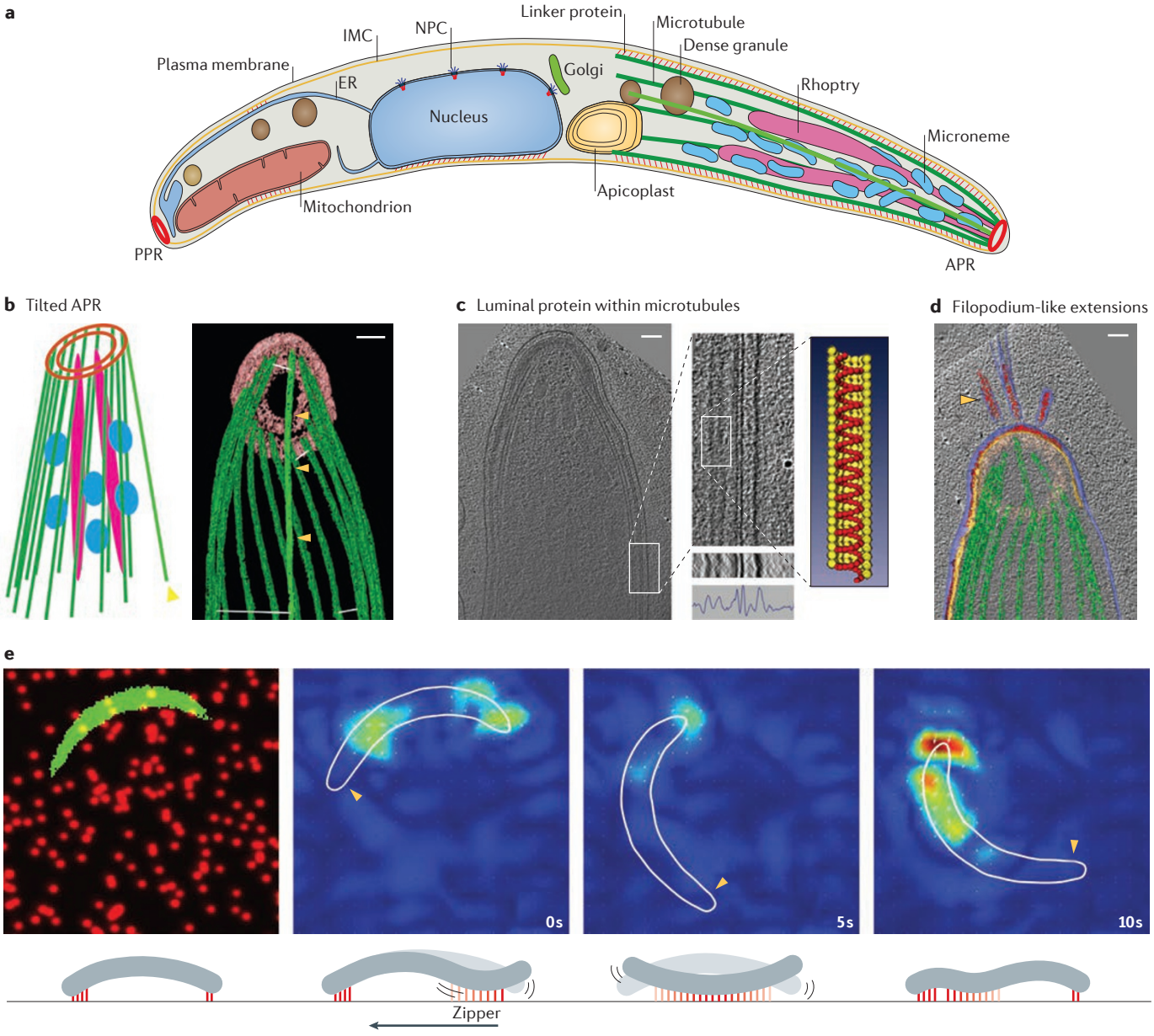

Highly sulfated proteoglycans
(HSPGs). A family of glycoproteins that are highly sulfated by covalently attached heparan sulfate chains. These glycoproteins are presented on the cell surface for ligand interaction and are found in all vertebrate tissues, but are highly enriched in the liver.

Cell traversal
Behaviour that is displayed by *Plasmodium* spp. sporozoites and ookinetes, involving the breaching of the plasma membrane of a host cell, gliding through the host cytosol and exiting the host cell.

One of the main findings achieved through the use of IVM was that *P. berghei* sporozoites are capable of using several pathways to cross the liver sinusoidal barrier en route to the hepatocytes[9,25] rather than translocating across the sinusoidal barrier exclusively through Kupffer cells (also known as the gateway model; BOX 1; see the figure, step 3)[46–48]. Using fluorescent *P. berghei* sporozoites that lack a protein that is essential for traversal (sporozoite microneme protein essential for traversal 2 (SPECT2))[49], in combination with control parasites and various reporters and dyes for endothelial and Kupffer cell integrity, spinning-disc confocal IVM revealed that sporozoites are able to cross the liver sinusoidal barrier by four different additional routes[9]: endothelial cell traversal following interactions with a Kupffer cell; endothelial cell traversal that is independent of interactions with Kupffer cells; an invasion–transcytosis variant of the gateway pathway, whereby sporozoites cross the barrier between a Kupffer cell and an adjacent endothelial cell; and crossing at a distance from Kupffer cells and without traversing endothelial cells. To explain this fourth form of crossing, two possibilities have been suggested: a paracellular pathway, whereby sporozoites cross between two endothelial cells, or a transcellular pathway, whereby sporozoites cross through endothelial cells but do not induce a loss of membrane integrity. Such a transcellular pathway is used by lymphocytes to cross the endothelium (reviewed in REF. 50). These findings not only disproved the previously accepted paradigm that the gateway model was the only method of sporozoite entry to the liver, but also indicated that about one-quarter of all crossing events are independent of cell traversal.

Development of* Plasmodium *spp. parasites within the liver. As a result of proteolytic processing of surface-exposed CSP, the motile sporozoites switch from the

◀ Figure 1 | **Imaging of *Plasmodium* spp. sporozoites. a** | Architecture of a mature sporozoite, showing organelles and specific architectural features that have been identified by cryoelectron tomography. These organelles include the posterior polar ring (PPR), the mitochondrion, the endoplasmic reticulum (ER), the inner membrane complex (IMC), the nuclear pore complexes (NPCs) and the nucleus, the Golgi apparatus, the apicoplast, the dense granules, the microtubules, the rhoptries, the micronemes and the apical polar ring (APR). **b** | Schematic (left panel) showing the inclined APR (red), the subpellicular microtubules (green; yellow arrowhead indicates the 'single' microtubule, which defines the dorsal side of the chiral sporozoite), the micronemes (cyan) and the rhoptries (magenta). A volume-rendered representation of an electron tomogram (right panel) clearly demonstrates the tilted APR and the 'single' microtubule (yellow arrowheads). White bars indicate distances between individual microtubules next to the APR and at 800 nm distance from the APR. Scale bar represents 100 nm. **c** | Electron tomography of a mature sporozoite, showing the projection of a 10-µm-thick section through the tomogram (left panel). The grey-scale intensity plot (bottom middle panel) shows the electron density peaks that correspond to (from the right) the plasma membrane, the IMC and a microtubule. The slope in the plot between the microtubule and IMC peaks corresponds to the thickened subpellicular network. A model of the microtubule (right panel) shows the luminal density (red), representing an unknown protein. Scale bar represents 100 nm. **d** | Filopodium-like extensions of the plasma membrane at the apical end of the sporozoite. The volume-rendered representation of a sporozoite shows three extensions (yellow arrowhead) of the plasma membrane (blue) with electron-dense material inside (red). The IMC (yellow) and the microtubules (green) are also shown. Scale bar represents 100 nm. **e** | Traction forces revealed by traction-force microscopy. The sporozoite (green) moves on a polyacrylamide gel loaded with fluorescent beads (red) to measure the traction force (top left panel). Plotting the data over time (three top right panels; red corresponds to high force, and blue corresponds to low force) illustrates the traction force that is exerted as the sporozoite (white outline) moves. The yellow arrow indicates how the contact between the sporozoite and substrate 'zips' backwards during motility, as illustrated in the schematic (bottom panel). The sporozoite depicted is 10 µm long. Part **a** is adapted with permission from REF. 138, Wiley. The left panel of part **b** is adapted from REF. 16. The right panel of part **b** is reproduced with permission from REF. 3, Wiley. The left and middle panels of part **c** are adapted from REF. 138, Wiley. The right panel of part **c** is reproduced from ©2007 Cyrklaff, M. *et al. J. Exp. Med.* **204**: 1281–1287. doi: 10.1084/jem.20062405. Part **d** is reproduced from REF. 16. Images in the top panel of part **e** courtesy of F.F. and J. Kratzer, University Hospital Heidelberg, Germany. The bottom panel of part **e** is reproduced from REF. 10, Elsevier.

transmigration to the invasion mode[43]. During the process of invasion, sporozoites induce the formation of a parasitophorous vacuole membrane (PVM; BOX 1; see the figure, step 5). The PVM represents the interface between the parasite and its host hepatocyte throughout liver-stage development, and it enables the parasite to scavenge nutrients by both passive diffusion through membrane pores and active transport[51–53]. One of the most relevant findings achieved by a combination of time-lapse imaging and fluorescence recovery after photobleaching (FRAP) was the extremely dynamic nature of the PVM[12,52]. Fluorescence tagging of the *P. berghei* proteins IBIS1 (REF. 52), UIS4 and EXP1 (REFS 12,52), which are transported to the PVM, enabled the characterization of the connectivity and spatiotemporal dynamics of the PVM and the host tubovesicular network (TVN), which is a microtubule-dependent membranous network. Remarkable findings included the observation of dynamic and motile PVM-derived and TVN-derived vesicles that spread throughout the host cell[54–57] (FIG. 2a; Supplementary information S4 (movie)).

Using long-term time-lapse imaging of sporozoite-infected HepG2 and HeLa cells and IVM of sporozoite-infected mouse livers, it was shown that the *P. berghei* PVM is recognized by the host cell autophagic machinery[12,58]. The labelling of the PVM by host autophagy markers was confirmed using super-resolution stimulated emission depletion (STED) microscopy[12]. Compared with electron microscopy-based methods, STED microscopy has the advantage that infected cells can be easily identified and analysed by fluorescence, rather than requiring cell sorting followed by extensive fixing and embedding procedures. Long-term time-lapse microscopy (for up to 72 hours) showed, for the first time, that the autophagic marker microtubule-associated protein 1 light chain 3B (LC3B) targets the PVM early in infection (FIG. 2b; Supplementary information S2 (movie)), followed by the elimination of most parasites, thereby uncovering a previously unknown cytosolic immune response[12] (FIG. 2b). By contrast, a surprising discovery was that during *P. berghei* schizogony (BOX 1; see the figure, step 6), successful parasites seem to actively remove autophagy marker proteins from the PVM, potentially by membrane shedding[12], and thus avoid continued attack by lysosomes (FIG. 2b, right panel). In contrast to selective autophagy, which can potentially eliminate the invading parasite, canonical autophagy is induced by starvation and can provide nutrients for essential cell functions. Indeed, quantitative confocal microscopy for measuring parasite sizes showed that the rapidly growing *Plasmodium* spp. parasite exploits canonical autophagy as an additional source of nutrients[12,58]. In addition to the success of IVM for imaging the *P. berghei* pre-erythrocytic developmental stages in terms of speed, time lapse and penetration depth, very recent work has obtained subcellular-resolution images of the parasite *in vivo*, enabling the visualization of previously unknown organelle structures in the developing parasite[5].

Another important observation achieved by wide-field fluorescence time-lapse microscopy was the highly dynamic host cell actin reorganization (or actin cloud formation) that takes place around developing *P. berghei* parasites 10–16 hours post-infection[59] (FIG. 2c; Supplementary information S5 (movie)). It has been proposed that gelsolin is necessary for severing actin filaments and, possibly, contributing to the dynamic actin turnover, which in turn might contribute to the mechanical confinement and/or elimination of the parasite. Thus, the observed reorganization of host actin has been suggested to be part of a broader defence strategy of the hepatocyte, such as autophagy.

Parasite egress from the liver. The final step of the pre-erythrocytic stage of *Plasmodium* spp. infection is egress from the liver hepatocytes and parasite release into the bloodstream (BOX 1; see the figure, steps 7–9). This transition from the liver to the blood stage was the final part of the pre-erythrocytic stage to be elucidated, and the process that was uncovered was one of the most exciting microscopy-based revelations of the past decade in the field of *Plasmodium* spp. liver-stage research. For many years, it was accepted that infected hepatocytes rupture to release progeny merozoites into the bloodstream to infect red blood cells (RBCs). However, this

Kupffer cells
Phagocytic cells, also known as resident stellate macrophages, that line the sinusoids of the liver.

Inner membrane complex
(IMC). An organelle of all alveolate organisms that consists of flattened vesicles which underlie the plasma membrane and are interconnected with the cytoskeleton.

Schizogony
A mode of asexual replication in which several rounds of mitosis generate a multinucleated cell. In *Plasmodium* spp., schizogony is followed by cytokinesis to form individual infectious merozoites.

Selective autophagy
Selective targeting of damaged cell organelles, large protein aggregates or intracellular pathogens for degradation in autophagosomes.

Canonical autophagy
An intracellular self-degradative process that delivers cytoplasmic constituents to the lysosome and is important for balancing sources of energy in response to nutrient stress or at key stages of cell development.

Gelsolin
An actin-binding protein that regulates actin filament assembly and disassembly.

UBC–eGFP mouse
A transgenic mouse that expresses enhanced GFP (eGFP) under the control of the ubiquitin C (*UBC*) promoter in all tissues.

assumption failed to explain how merozoites reach the bloodstream, as even following liver cell rupture, merozoites would still be extravascular. Unlike sporozoites, merozoites cannot use typical gliding motility to transmigrate endothelial cells. Long-term time-lapse live imaging of *P. berghei*-infected hepatocytes *in vivo* and *in vitro* revealed that after PVM rupture, released merozoites move freely in the host cell cytoplasm and this is followed by the initiation of host cell death[45,60] (BOX 1; see the figure, step 7). The delayed rupture of the host cell plasma membrane enables the formation of merozoite-filled membranous bodies that were hence named merosomes[45] (BOX 1; see the figure, step 8; FIG. 2d; Supplementary information S6 (movie)). To further characterize host cell death during merosome formation, fluorescence-based detection of phosphatidylserine residues was used[45,60], because phosphatidylserine residues act as generic 'eat me' signals of apoptotic cells to attract phagocytic macrophages. In contrast to phosphatidylserine-positive apoptotic cells, the plasma membrane of merosomes remains phosphatidylserine-negative, which indicates that the observed cell death of infected

Box 2 | **Intravital imaging of *Plasmodium* spp. parasites in rodents**

Intravital microscopy (IVM) is a powerful tool for addressing questions regarding the dynamics of cellular and immunological processes under physiological conditions. Recent advances in IVM include improved microscope design and optics; organ windows to minimize motion artefacts; anaesthetics to improve survival; and improved software for image analysis. There are several ways to image the deep tissues and cellular processes of a living animal after the surgical exposure of organs: injection of fluorescently labelled probes; transient expression of fluorescently labelled molecules; or the use of transgenic reporter mice and fluorescently labelled *Plasmodium* spp. parasites (see the figure, part **a**). Several examples of such imaging are described below and illustrated in the figure. Quantitative skin IVM following a mosquito bite and injection of sporozoites shows the blood vessels of a transgenic mouse expressing fetal liver kinase 1 (FLK1; also known as VEGFR2)–GFP, highlighting the blood vessel endothelial cells (green), traversed cells (red) and the projection of 4 minutes of sporozoite motility in the skin (white; see the figure, part **b**). Liver IVM of a transgenic mouse expressing microtubule-associated protein 1 light chain 3B (LC3B)–GFP and infected with an mCherry-expressing *Plasmodium berghei* parasite shows microtubules in the host liver cells (green) and merosome formation by the parasite (red; see the figure, part **c**). Brain IVM imaging has shown macrophages (green) recruited to post-capillary venules (red) in *P. berghei* ANKA-infected mice (see the figure, part **d**). Spleen remodelling and splenomegaly have been well characterized in lethal and non-lethal human and rodent malaria. The great vascularization of the spleen and the fast circulation of blood demand the use of high-speed time-lapse microscopy to view this tissue, and this technique has revealed the spleen vasculature of a *UBC*–eGFP mouse (green) infected with *P. berghei* ANKA parasites (red; see the figure, part **e**). Various imaging platforms have shown the preferential accumulation of *Plasmodium* spp. parasites in the vessels of the adipose tissue; for example, viewing abdominal adipose tissue of *UBC*–eGFP mice infected with mCherry-expressing *P. berghei* ANKA parasites (see the figure, part **f**).

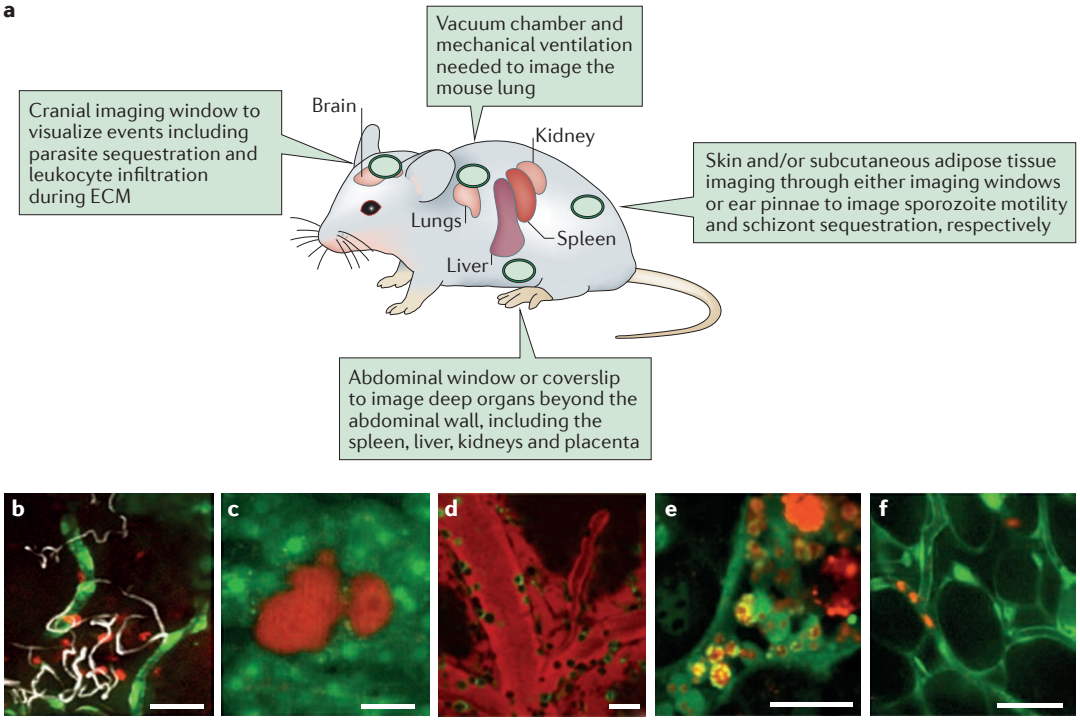

Scale bars represent 20 μm. ECM, experimental cerebral malaria. Image in part **b** courtesy of R. Amino and P. Formaglio, Institut Pasteur, Paris, France. Image in part **c** courtesy of V.T.H. and N. Eickel, University of Bern, Switzerland. Part **d** is reproduced from REF. 137. Images in parts **e**,**f** courtesy of V.T.H. and M.D.N.

hepatocytes is ordered but is not typical apoptosis. Thus, patrolling macrophages and neutrophils are unable to recognize the migrating phosphatidylserine-negative merosomes. Merosome budding from infected hepatocytes through the endothelial layer into the blood vessel has been demonstrated by versatile quantitative IVM techniques[45] (BOX 2; see the figure, part **c**). Importantly, merosome formation seems to be a conserved egress strategy of *Plasmodium* spp., as similar structures to those identified in *P. berghei* infections have been observed in *Plasmodium yoelii* infection[47] and in *Plasmodium falciparum*-infected immunocompromised mice engrafted with human hepatocytes[61].

The asexual blood stages

Following the migration of merosomes into the liver vasculature and transport to the lung capillaries[47], merozoites are released into the circulation (BOX 1; see the figure, step 9), which marks the beginning of the blood stage. Following invasion of an RBC by the merozoite, the intra-erythrocytic parasite life cycle is divided into ring, trophozoite and schizont stages, eventually leading to the release of 16–32 daughter merozoites, which invade new RBCs to begin the cycle again (BOX 1; see the figure, step 13). Each cycle results in RBC rupture and the induction of periodic waves of fever in infected patients. Blood-stage parasites modify their host cell in a process that is dependent on the export of numerous parasite proteins into the RBC. Host cell modifications are necessary for the intracellular survival of the parasite. These changes include altered permeability of the RBC membrane to nutrients and the creation of host cell surface structures termed knobs, which facilitate the virulence factor display that is necessary for the sequestration of infected RBCs (reviewed in REF. 62). One prominent host cell modification in the cytoplasm of infected RBCs is the formation of Maurer's clefts, which are parasite-induced membranous organelles that are involved in the sorting of parasite proteins in the host cell and are key for the delivery of virulence factors to the surface of the infected erythrocyte[63] (BOX 1; see the figure, steps 11–12). These virulence factors mediate parasite sequestration to the vascular endothelium of several organs of the host (BOX 2; see the figure, parts **d**–**f**).

Imaging the erythrocytic cycle and host cell remodelling. Previously, phototoxicity and lysis of the acidic food vacuole of the parasites had made it impossible to view the entire *P. falciparum* blood stage at the level of individual parasites[64]. However, a recent investigation used confocal fluorescence and differential interference contrast (DIC) microscopy linked with photoconversion to study for the first time the development and concomitant host cell modifications in individual erythrocytic stages of the parasite (FIG. 3a; Supplementary information S7, S8 (movies))[11]. In this new study, 4D imaging revealed two unexpected findings regarding host cell remodelling, protein export and Maurer's clefts. A large body of research has provided crucial insights into the architecture, function and morphology of Maurer's clefts, as well as their role in protein trafficking. Previous studies proposed that parasite membrane proteins are exported to Maurer's clefts by insertion into the nascent clefts at the PVM, thereby linking the biogenesis of Maurer's clefts to protein export[65–69] (recently reviewed in REF. 70). The first unexpected finding revealed by 4D imaging was that Maurer's clefts do not constantly form from the PVM, as was previously believed, but rather that the total number of Maurer's clefts is already present shortly after parasite invasion and remains constant throughout the entire erythrocytic cycle until shortly before parasite egress[11]. These findings suggest that proteins that are destined for export are trafficked to already formed Maurer's clefts. Moreover, photoconversion combined with 4D imaging revealed the arrival of new cargo at the Maurer's clefts[11]. This implies that protein export must occur through soluble intermediates[71], or possibly also through vesicles trafficking between the PVM and the Maurer's clefts[72], rather than by insertion into the clefts at the PVM, as proposed by the nascent-cleft hypothesis. The second previously unknown phenomenon shown by 4D imaging was that segmentation of progeny merozoites following schizogony (BOX 1; see the figure, step 12) coincides with the collapse of Maurer's clefts, which might indicate that the parasite-induced structures in the host cell are dismantled, perhaps to facilitate egress[11] (BOX 1; see the figure, step 13).

In RBCs that contain ring-stage parasites (BOX 1; see the figure, step 10; FIG. 3a), the Maurer's clefts show rapid movement in the cytoplasm[11]. Concomitant with the transition of the parasites to the trophozoite stage (BOX 1; see the figure, step 11; FIG. 3a), the Maurer's clefts become anchored to the RBC cytoskeleton[11]. Cryoelectron tomography and fixed-cell electron tomography imaging techniques have provided two competing but not mutually exclusive ideas of how the Maurer's clefts attach to the RBC plasma membrane and/or cytoskeleton. One research group suggested that attachment is mediated by stalk-like structures called tethers[73–76], whereas a different group proposed that this connection is mediated by host actin filaments[4] (FIG. 3b). Both of the structures seen contained attached vesicles and could, in principle, act as cables for virulence factors that traffic from the Maurer's clefts to the host cell surface. Electron tomography of parasites in RBCs from patients with sickle cell disease and of a parasite line lacking a Maurer's cleft protein showed ablated surface display of virulence factors and a disrupted state of the Maurer's clefts–actin organization[4,77]. These images provided the first molecular insights into how parasite proteins are trafficked over the last hundred nanometres en route to the RBC plasma membrane.

Merozoite attachment to and invasion of host red blood cells. Merozoite invasion and egress (BOX 1; see the figure, steps 9, 13; FIG. 3c,d) are widely studied topics in the field of malaria research, but real-time imaging of these events had been hindered by poor merozoite viability, their small size (1–3 μm), their susceptibility to photo-damage and the speed of these processes. Despite their small size, merozoites contain all of the organelles that are necessary to attach to and invade

Knobs
Protrusions, or knob-like raised platforms, on the surface of *Plasmodium falciparum*-infected red blood cells. These knobs are formed by the self-assembly of the parasite protein knob-associated histidine-rich protein (KAHRP) and enable the presentation of erythrocyte membrane protein 1 (PfEMP1).

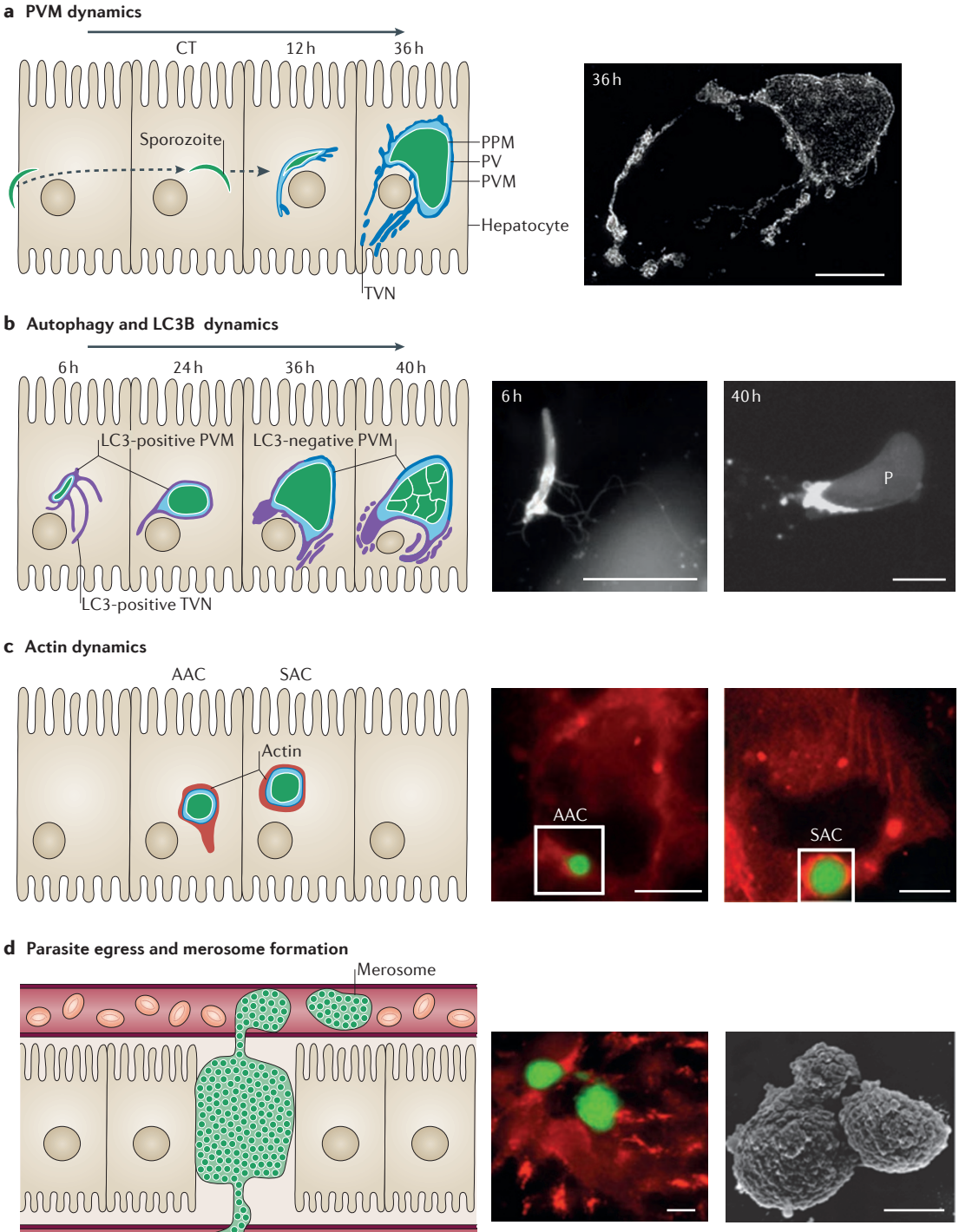

Rhoptries
Specialized secretory organelles that are positioned at the apical end of certain stages of apicomplexan parasites, including *Plasmodium* spp. sporozoites and merozoites. They have a function in host cell invasion and the formation of the parasitophorous vacuole membrane.

Dense granules
Specialized secretory organelles that are positioned at the apical part of certain stages of apicomplexan parasites, including *Plasmodium* spp. sporozoites and merozoites. They are involved in host cell modification during invasion.

Micronemes
Specialized secretory organelles that are positioned at the apical end of apicomplexan parasites, including all motile *Plasmodium* spp, stages. They function in host cell adhesion and motility.

RBCs. Invasion-related organelles that are present in the merozoite include rhoptries, dense granules and micronemes[15,78]. Various imaging methods, including time-lapse DIC and fluorescence microscopy, optical tweezers, super-resolution microscopy, cryo-electron tomography and cryo-X-ray tomography, have led to a better understanding of the molecular mechanisms and kinetics that mediate merozoite attachment and invasion. Time-lapse microscopy studies revealed three distinct phases of *P. falciparum* invasion[6] (BOX 1; see the figure, step 9; FIG. 3c). In the first phase, merozoites make contact with the RBC, triggering waves of deformation in the RBC emanating from the contact site. This phase ends with the reorientation of the merozoite, bringing its apical pole, in which the secretory organelles are located, into contact with the erythrocyte surface. At this point, the merozoite is irreversibly attached to the erythrocyte surface and committed to invasion[6].

◀ Figure 2 | **Imaging techniques reveal relevant biological events during liver-stage development. a** | Schematic images (left panel) of the parasitophorous vacuole membrane (PVM) at early (12 hour) and late (36 hour) time points post-infection. Sporozoites traverse several cells (cell traversal; CT) before undergoing a switch to invade. On invasion, the parasite induces the formation of a PVM. Time-lapse imaging, photo-activation and super-resolution microscopy have shown the PVM and the host tubovesicular network (TVN) to be extremely dynamic, with tubules and vesicles extending large distances into the host cell, away from the parasite body. The parasite plasma membrane (PPM) and parasitophorous vacuole (PV) are indicated. The confocal image (right panel) shows the PVM of a *Plasmodium berghei* liver-stage parasite 36 hours post-infection; scale bar represents 50 µm. **b** | Schematic form of host cell microtubule-associated protein 1 light chain 3B (LC3B; purple) dynamics with respect to the *P. berghei* parasite throughout infection, including heavy accumulation at early time points and lateral localization of LC3B at late time points post-infection. Microscopy shows host cell LC3B accumulations around an invaded *P. berghei* sporozoite early post-infection (middle panel), and LC3B localization to the lateral side of the PVM (away from the *P. berghei* schizont; P) and to TVN vesicles later post-infection (right panel). Scale bars represent 10 µm. **c** | Schematic (left panel) and wide-field fluorescence microscopy images (middle and right panels) of the dynamics of host cell actin clouds around developing *P. berghei* liver-stage parasites. Asymmetrical and symmetrical actin clouds (AACs and SACs, respectively; actin is labelled red) are present around GFP-tagged *P. berghei* (green). Scale bars represent 10 µm. **d** | Schematic of merosome formation during parasite egress (left panel). Spinning-disc confocal intravital imaging of liver tissue infected with GFP-tagged *P. berghei* shows the parasite undergoing merosome budding and egress into the sinusoidal vessel (middle panel). Red fluorescent BSA was used to label the blood vessels. Scanning electron microscopy shows budding *P. berghei* merosomes (right panel). Scale bars represent 10 µm. Confocal microscopy image in part **a** courtesy of V.T.H. and C. Agop-Nersesian, University of Bern, Switzerland. Microscopy images in part **b** courtesy of V.T.H. (left and right images) and N. Eickel, University of Bern, Switzerland (left image). Microscopy images in part **c** adapted from REF. 59. Part **d** is adapted from Sturm, A. *et al.* Manipulation of host hepatocytes by the malaria parasite for delivery into liver sinusoids. Science **313**, 1287–1290 (2006). Reprinted with permission from AAAS.

A combination of imaging techniques, including cryo-electron tomography, cryo-X-ray tomography and super-resolution structured illumination microscopy (SIM), have shown that irreversible attachment of the merozoite to the RBC is mediated by erythrocyte-binding ligands (EBLs) and reticulocyte protein-binding homologues (RHs) on the surface of the parasite[7,74,79–83]. It is noteworthy that cryo-X-ray tomography provided 3D nanoscale information about the localization of molecules within cells in their native state. This is the only technique that can provide information at this resolution about unstained, whole cells thicker than 1 µm and that can combine the power of light, electron and X-ray microscopes.

In the second phase of invasion, the merozoite enters the RBC in a process that is dependent on an actin–myosin (actomyosin) motor and the formation of a tight junction at the interface between the merozoite and erythrocyte plasma membranes[7,84,85]. SIM demonstrated an RBC receptor-independent mode of host cell adhesion through the parasite ligand apical membrane antigen 1 (AMA1)[7]. The merozoite secretes the rhoptry neck (RON) complex of proteins, and RON2 acts as an anchor in the erythrocyte membrane for RON complex assembly and AMA1 engagement[7,85,86]. AMA1 and RON proteins were found to colocalize at the tight junction during invasion. Importantly, inhibition of the AMA1–RON interaction prevents merozoite invasion[87]. Although these findings are supported by some genetic studies, other genetic data are contradictory, and it is possible that this model for AMA1 function is too simplistic[88–91]. In terms of the relevance of imaging for the elucidation of the aforementioned interactions, super-resolution microscopy provides various techniques for imaging other *Plasmodium* spp. stages, but thus far SIM is the only super-resolution microscopy technique to be regularly used for imaging the blood stages[7]. SIM is compatible with live cell imaging, given that it requires only low illumination intensities, can rapidly acquire large fields of view and can take advantage of most existing fluorophores[92]. However, compared with some other super-resolution techniques such as STED, stochastic optical reconstruction microscopy (STORM) or photoactivated localization microscopy (PALM), the resolution gain over conventional fluorescence microscopy is comparably low.

The third phase of invasion occurs 10–20 seconds after the merozoite fully enters the erythrocyte and is characterized by echinocytosis of the RBC, whereby the edges of the RBC curl and fine spicules are formed. It was hypothesized that this process is triggered by the resealing of the erythrocyte plasma membrane behind the merozoite[6].

An important finding achieved through the use of optical tweezers was that the different steps in invasion are independent[93]. Placing dead merozoites close to RBCs using optical tweezers showed that merozoites which had lost the ability to invade 2–3 minutes post-egress nonetheless retain the ability to adhere to RBCs and still induce transient local membrane deformations in the RBC membrane. A contribution of the RBC membrane to merozoite invasion was also suggested using computational modelling[94], an approach that is likely to be used more frequently to complement quantitative imaging in future studies.

Egress from host red blood cells. The final step of the erythrocytic cycle is the release of invasive merozoites on rupture of the infected erythrocyte (BOX 1; see the figure, step 13; FIG. 3d). Parasite release from the host RBC requires the opening of the PVM and RBC membranes. DIC imaging showed that before egress, the parasites move freely in the RBC following rupture of the PVM, while the RBC membrane is still intact[95]. Time-lapse microscopy using calcium and fluorescence imaging further demonstrated the involvement of parasite proteases and perforin-like proteins in increased osomolarity[96] and revealed that Ca^{2+}-dependent permeabilization and membranolytic activities are necessary for merozoite release. Although it was previously believed that merozoite egress was an explosive event, recent studies using high-speed DIC video microscopy and epifluorescence imaging showed that egress is in fact an ordered process, beginning with the opening and stabilization of an osmotic pore in the RBC membrane[95] (FIG. 3d). High-speed imaging indicated that after osmotic swelling of the infected RBC, lasting 400–800 milliseconds[95], and rupture of the PVM, three steps lead to egress: an initial phase termed osmotic

Myosin
A large family of ATP-dependent motor proteins that bind to and translocate cargo along actin filaments.

Echinocytosis
The formation of an abnormal cell membrane with multiple small, evenly spaced projections. This phenomenon is unique to red blood cells and is often induced by *Plasmodium* spp. invasion.

a Time-lapse imaging of *P. falciparum* blood stages

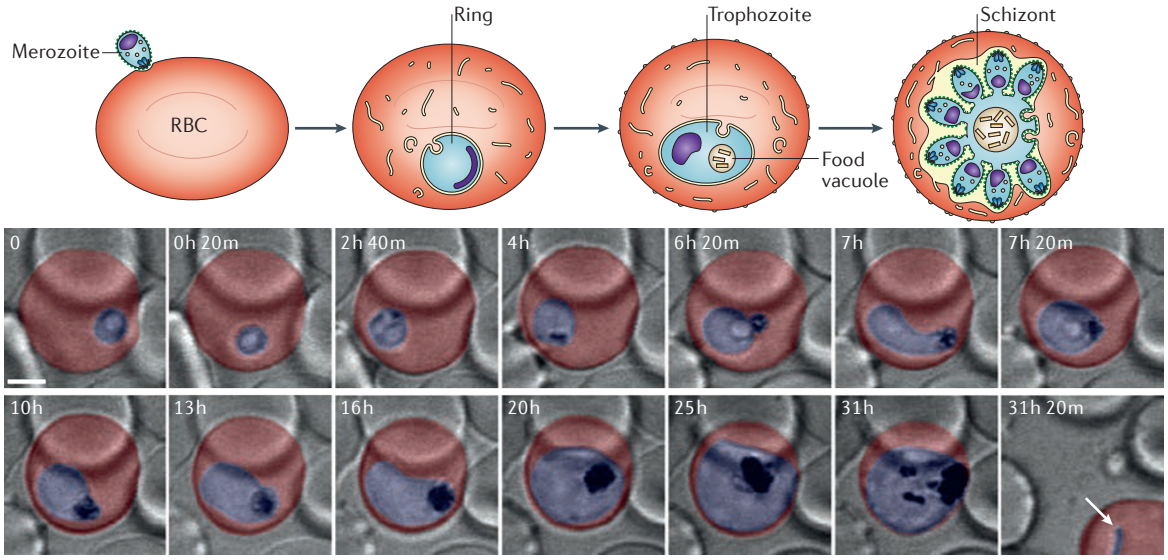

b Imaging the architecture of Maurer's clefts

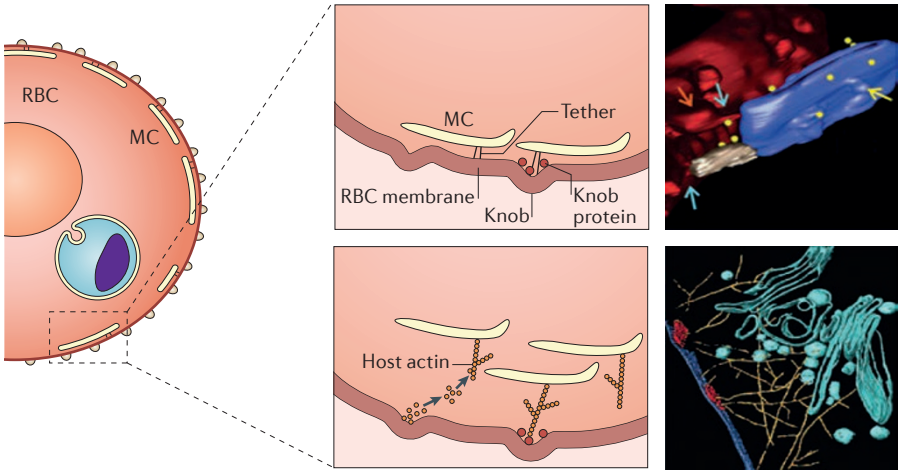

c Merozoite invasion

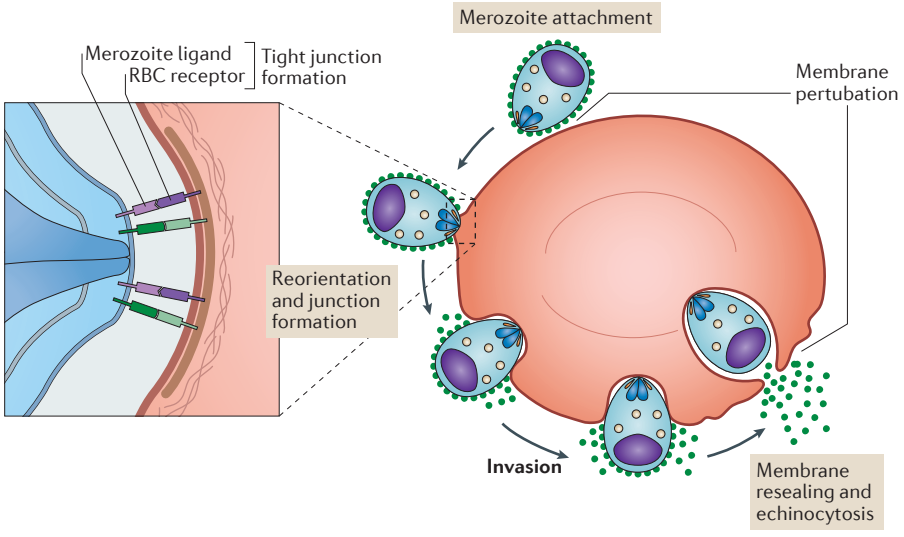

d Merozoite egress

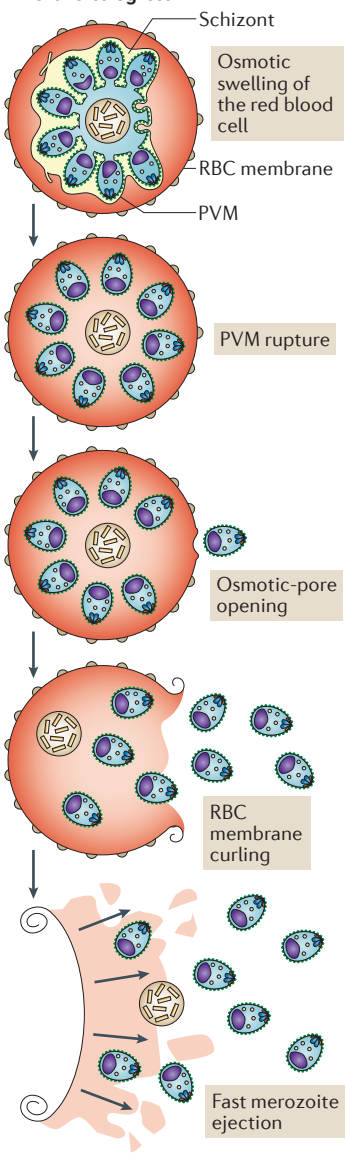

Figure 3 | **Imaging of *Plasmodium* spp. erythrocytic stages. a** | Graphic representation of the four main blood stages of *Plasmodium* spp. development (upper panel), and 4D imaging of the developing *Plasmodium falciparum* parasite (blue) using confocal microscopy (lower panel), showing the complete erythrocytic stage of development in an individual red blood cell (RBC; red). Selected time points in differential interference contrast (DIC) microscopy are shown, from ring stages to schizont stages. The white arrow at 31 h 20 m shows a ring stage derived from reinvasion after rupture. Scale bar represents 2 µm. **b** | Maurer's clefts (MCs) at the RBC membrane. One study indicates that Maurer's clefts attach to the host cell membrane through stalk-like tethers, as illustrated in the schematic (top left). A volumetric reconstruction and rendering of the immuno-electron tomograms (top right) shows a tether-like structure (grey) connecting a Maurer's cleft (blue) to the RBC membrane (red). Regions that may represent RBC cytoskeleton extensions are indicated with cyan arrows. Thickening of the Maurer's cleft coat is observed in some regions and is indicated with a yellow arrow. Bulge in the RBC membrane is indicated by a red arrow. A second study found evidence that the attachment is instead mediated by host actin filaments, as illustrated (bottom left). A surface-rendered cryoelectron tomogram of a *P. falciparum*-infected erythrocyte (bottom right) shows a network of long branched actin filaments (yellow) connecting the Maurer's clefts (cyan) to the knobs (red) and the plasma membrane (dark blue); 20–200 nm vesicles (cyan) are also attached to these filaments**. c** | The three steps of invasion observed by time-lapse imaging, and details of the receptor–ligand interactions as defined by super-resolution microscopy[7]. During the first step of invasion, merozoite attachment induces perturbations in the RBC membrane. This step ends in the merozoite reorienting to bring its apical end in contact with the RBC membrane. In the second step, a tight junction is formed, mediated by erythrocyte receptors and parasite ligands. Penetration of the parasite into the RBC is mediated by an actomyosin motor. Following complete invasion, the third step involves resealing of the RBC membrane and RBC echinocytosis. **d** | High-speed DIC time-lapse microscopy enabled the identification of a series of ordered events that are involved in merozoite egress[95]. In the mature schizont, osmotic pressure increases before rupture of the parasitophorous vacuole membrane (PVM). Following PVM rupture, the merozoites are able to move freely in the RBC while the RBC membrane remains intact. An osmotic pore is then formed in the RBC membrane, during which an osmotic release of 1–2 merozoites occurs in a matter of milliseconds. After this, the RBC membrane curls and then 'buckles', dispersing all remaining merozoites in multiple directions up to 10 µm away, towards neighbouring RBCs. Microscopy images in part **a** are from REF. 11, Nature Publishing Group. Top right image in part **b** is adapted with permission from REF. 139, Wiley. Bottom right image in part **b** is adapted from Cyrklaff, M. *et al.* Hemoglobins S and C interfere with actin remodeling in *Plasmodium falciparum*-infected erythrocytes. *Science* **334**, 1283–1286 (2011). Reprinted with permission from AAAS. Part **c** is adapted with permission from REF. 82, National Academy of Sciences.

release, whereby 1 or 2 merozoites are released in the first 100–200 milliseconds, followed by two steps of 'inelastic release', whereby the RBC membrane changes its curvature and buckles, liberating the remaining merozoites in a dispersing manner. This form of egress and dispersion is believed to be necessary to optimize merozoite invasion of neighbouring RBCs up to 10 µm away from the RBC of origin.

The sexual blood stages

Asexual replication of blood-stage parasites results not only in the multiplication of parasite numbers in the blood, but also in the generation of gametocytes (BOX 1; see the figure, step 14) for transmission to the definitive host (that is, the mosquito vector; BOX 1; see the figure, step 15). Interestingly, only very early (stage I) and mature (stage V) *P. falciparum* gametocytes are found in human blood circulation (BOX 1; see the figure, step 14), whereas immature forms (that is, stages II–IV) are absent from the circulation and instead sequestered in the bone marrow and spleen, as confirmed by ultrastructural analysis[97] (FIG. 4a).

Whereas the sequestered immature gametocyte stages are rigid, it is thought that a switch in RBC and gametocyte deformability occurs in the final stage of gametocyte maturation, rendering mature gametocytes (and their associated RBCs) more flexible; the presence of mature gametocytes in the circulation is thought to be a direct consequence of this switch. 3D live imaging in capillary assays *in vitro* and 3D finite-element whole-cell modelling were used to study the circulatory characteristics of *P. falciparum* gametocytes at different stages of maturation[98–100] and the role of cellular deformability during circulation in the blood[100] (FIG. 4b). The simulations that were generated from these studies led to the hypothesis that the morphological and biophysical changes in the gametocyte-infected RBC are linked to tissue distribution *in vivo*, as only RBCs that contain either very early (stage I), and thus small, or mature (stage V) gametocytes could easily traverse the splenic interendothelial slits under physiological pressure; RBCs infected with stage II–IV gametocytes would be unable to squeeze through the slits and would be trapped in the spleen. This ensures the survival of the mature gametocytes so that they can be taken up by the mosquito during a blood meal (BOX 1; see the figure, step 15). The spleen is generally regarded as a central organ in malaria pathology (reviewed REFS 101–104) owing to its capacity to eliminate RBCs with reduced deformability, including infected RBCs. The function of the spleen is thought to have driven *Plasmodium* spp. to evolve mechanisms to avoid splenic passage and sequestration. To date, the presence of gametocytes in the spleen and the effect this might have on transmission and overall parasite biology are being investigated.

Cryo-X-ray microscopy led to the first detailed observation of changes in the subpellicular membrane complex (a membrane structure that is underpinned by a layer of microtubules) as gametocytes mature. The extension of this subpellicular complex drives parasite and host cell elongation and is responsible for the characteristic crescent shape of *P. falciparum* gametocytes. 3D SIM imaging uncovered new details about the organization and function of the actin cytoskeleton in gametocytes[98,105–107]. Actin polymerization has been previously described as necessary for the motility of apicomplexan parasites, so the discovery of polymerized actin in non-motile gametocytes was very surprising. The structures that contain F-actin in gametocytes constitute a previously unrecognized actin-based cytoskeleton that seems to be assembled very early in gametocyte development. This cytoskeleton provides a template for the positioning of microtubules and stabilizes the tubulin cytoskeleton[107]. 3D SIM demonstrated the accumulation of such structures at the poles of the gametocyte, radiation into the parasite body and close association with the tubulin cytoskeleton (FIG. 4c).

Outlook

Over the past decade, technical advances in imaging techniques have enabled extraordinary studies of *Plasmodium* spp. biology and host–pathogen interactions. It is safe to

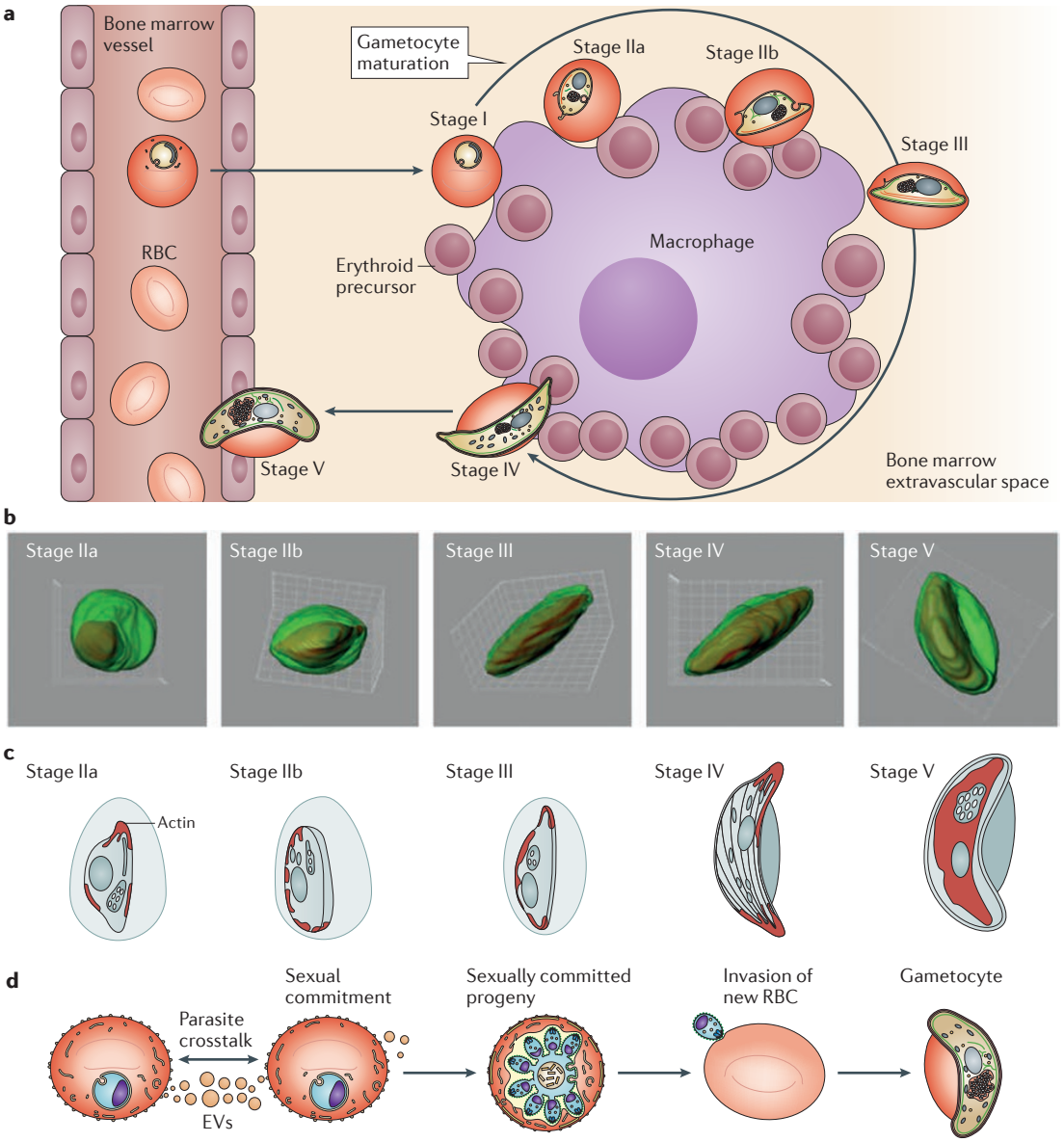

Figure 4 | **Imaging of the architecture, deformability and sublocalization of *Plasmodium* spp. sexual stages within the host bone marrow. a** | Autopsy studies showed that immature gametocytes are found mainly in the extravascular space of the bone marrow, where they are preferentially localized in the vicinity of erythroblastic islands (which are nursing macrophages in which erythroblasts and other erythroid precursors localize) and develop within erythroid precursors. Stages I – IV remain within the extravascular space, whereas stage V gametocytes undergo a deformability switch and are able to re-enter the peripheral circulation, where they can be taken up by mosquitoes. **b** | Model geometry from a 3D analysis of gametocyte development. Morphological differentiation of the parasite causes substantial deformation of the host red blood cell (RBC), transforming it from a discoidal to an elongated ellipse as the gametocyte matures from stage II to stage V. **c** | Imaging studies have found unexpected localization of F-actin in *Plasmodium falciparum* gametocytes. F-Actin (red) accumulates at the gametocyte tips and at the parasite periphery in early-stage gametocytes. The transition to mature stage V gametocytes is accompanied by the coordinated disassembly of the microtubule and F-actin cytoskeletons, leading to a more diffuse labelling pattern[107]. **d** | Extracellular vesicles (EVs; such as microvesicles and exosomes) that are derived from infected erythrocytes mediate cellular communication within the parasite population and are thought to stimulate the production of transmission-stage parasites. Part **b** is adapted with permission from REF. 100, Wiley.

Mesoscopic imaging
An imaging modality with penetration depths of up to 10 mm and resolutions of below 100 μm, depending on the tissue type and wavelength of operation. Examples include fluorescence tomography and optoacoustic imaging.

assume that imaging methods will remain prominent in malaria research in the future, for two reasons. First, the new techniques that have been introduced to date, such as super-resolution microscopy, cryoelectron tomography and IVM, have not yet been fully exploited for malaria research. Second, other recently developed imaging techniques, such as those involving mesoscopic imaging, will surely be applied in the field in the years to come.

Microvesicles and exosomes
Forms of extracellular vesicle that represent an important mode of intercellular communication and are capable of transferring cytosolic proteins, lipids and RNAs between cells. Although a precise definition for each type of vesicle is lacking, exosomes are typically characterized as < 100 nm, whereas microvesicles are defined as 100–1,000 nm.

Hypnozoites
Liver-stage parasites (*Plasmodium vivax* or *Plasmodium ovale*) that enter a latent, non-replicative state shortly after hepatocyte invasion. These dormant hypnozoites can be reactivated to complete liver-stage development thus causing a blood-stage infection in the range of weeks to years after an initial infection.

One key challenge in malaria research is to dissect the molecular details of the different life cycle stages of the parasite. Resolution down to single molecules has been achieved by cryoelectron tomography, but the thickness of the specimens that can be analysed is currently restricted to less than 1 µm. Hence, cryoelectron tomography has only been used to explore sporozoite architecture and the role of the host cell cytoskeleton at the edge of infected RBCs. Further improvements in this technique[108,109] will enable the investigation of thicker parasite forms, such as oocysts, later liver-stage parasites and perhaps schizont-infected RBCs. Correlative light and electron tomography[110] provides great opportunities for dynamic imaging, for instance to study the changes in cytoskeleton architecture during gliding motility of sporozoites. Depending on the freezing procedure that is required, it should theoretically be possible to image the same sporozoite in different migration phases.

Other underexplored topics in malaria research are signalling pathways in the parasite and the host cell. These cannot be approached solely by biochemical means, as an understanding of signalling at a single-cell level, in particular during liver-stage development, is necessary. A biochemical approach would be limited because only a small percentage of hepatocytes are infected, and not every parasite develops successfully. As signalling events are often very fast, imaging methods such as spinning-disc microscopy, light sheet microscopy[111–113] and holographic high-speed imaging[114] — in combination with a series of FRET-based signalling reporter constructs that are now available for mammalian cells[115] — would be needed to further increase our understanding of these events in infected cells. To this end, optogenetic tools that enable the triggering of signalling processes by light will also prove beneficial[116].

Phototoxicity is a major problem in live imaging approaches owing to the energy that is required to excite the fluorescent dyes. Exposure times can be limited through the use of ultrafast imaging techniques in combination with highly sensitive cameras that capture maximum numbers of photons. A different approach that might revolutionize live cell microscopy is lattice light sheet microscopy[117]. This method combines the advantages of super-resolution SIM microscopy with markedly reduced levels of photo-damage, achieved by the use of a multiple-beam approach applied to light sheet microscopy. This non-invasive high-speed 4D imaging enables single molecules to be followed in living cells. In combination with the nascent technology of small-molecule labelling (which enables the tagging of proteins that are refractory to fusion with large fluorescent proteins), these new techniques should facilitate the dissection of most cellular processes[118,119].

Another technique with interesting potential in terms of high resolution and speed is atomic-force microscopy (AFM). AFM has greatly facilitated the study of the infected-erythrocyte surface and in particular has enabled a detailed analysis of the 30–40 nm knobs on the surface of *P. falciparum*-infected RBCs[120–123]. Other applications of AFM have included investigations of RBC cytoadherence and parasite sequestration. These included functionalization of cantilevers to attach host receptors to which erythrocyte membrane protein 1 (PfEMP1) binds, and measure the force of interaction that is relevant to sequestration of the parasite[124,125]. Surface topography and receptor–ligand interactions have been extremely valuable applications, but, over the past decade, progress in AFM has also enabled real-time high-speed imaging of living cells. Although high-speed AFM is challenging because of the time of collision between the cantilever and the sample, various techniques have been implemented, one of which relies on the attachment of extremely long and thin tips by amorphous carbon to the cantilever[126,127]. Because of its versatility, AFM is regarded as a 'lab on a tip', capable of simultaneously providing information about the structure and the biological, chemical and physical parameters of whole living cells or individual molecules[128]. AFM has also been used to identify microvesicles and exosomes generated by infected RBCs[129]. Microvesicles act as a means of communication among *Plasmodium* spp. parasites. In 2014, two independent studies showed that following internalization by infected RBCs, these microvesicles stimulate conversion and commitment to the sexual parasite cycle[129,130] (FIG. 4d). These findings have important implications for cell–cell communication, as the process is reminiscent of quorum sensing displayed by other organisms and might be relevant for research developing methods to block malarial transmission[129,130]. The microvesicle field is currently in its infancy but has already attracted major attention owing to its potential application in vaccine development[131] and its relevance to disease transmission[129,130], and imaging methods to study the generation and the fate of the microvesicles are likely to provide further insights in this emerging field.

Regarding the transmission stages of *Plasmodium* spp., high-resolution imaging of gametocytes led to the identification of structures similar to those relevant for motility and invasion in sporozoites and merozoites[107]. This is an interesting aspect, as the preferential localization of gametocytes seems to be the extravascular space of the bone marrow, but it is not known how they cross the endothelium to reach this location. The elucidation of gametocyte migration in the bone marrow is therefore a next step to address in the field.

Although IVM and animal imaging advances are not addressed exhaustively in this Review, an enormous amount of progress has been achieved in this field, some of which has been translated to malaria research using rodent models. In addition, remarkable headway has been made in the past few years in developing humanized mouse models for *in vivo* studies of human diseases, offering an unprecedented balance between human species-specific tissues and cells, and a small vertebrate model[132–135]. Of relevance to malaria research, progression through the complete *P. falciparum* life cycle is now possible in humanized mice[133,134], and the formation of hypnozoites and invasion of reticulocytes by *P. vivax* have also been achieved using these models[135]. Together with the suite of imaging techniques and discoveries reviewed here in mice, extrapolation to human infections is now feasible in these models.

Finally, as imaging techniques progress and quantitative imaging becomes more important for the malaria field, advances in image processing and analysis software, as well as improvements in data storage, have become equally necessary. Undoubtedly, in the decades to come, further advances in imaging tools will play a key part in improving our understanding of the malaria parasite in terms of its basic biology, pathology and host–pathogen interactions.

1. World Health Organization. *World Malaria Report* (WHO, 2015).
2. Cyrklaff, M. *et al.* Cryoelectron tomography reveals periodic material at the inner side of subpellicular microtubules in apicomplexan parasites. *J. Exp. Med.* **204**, 1281–1287 (2007).
3. Kudryashev, M. *et al.* Structural basis for chirality and directional motility of *Plasmodium* sporozoites. *Cell. Microbiol.* **14**, 1757–1768 (2012).
4. Cyrklaff, M. *et al.* Hemoglobins S and C interfere with actin remodeling in *Plasmodium falciparum*-infected erythrocytes. *Science* **334**, 1283–1286 (2011).
5. Kaiser, G. *et al.* High resolution microscopy reveals an unusual architecture of the *Plasmodium berghei* endoplasmic reticulum. *Mol. Microbiol.* http://dx.doi.org/10.1111/mmi.13490 (2016).
6. Gilson, P. R. & Crabb, B. S. Morphology and kinetics of the three distinct phases of red blood cell invasion by *Plasmodium falciparum* merozoites. *Int. J. Parasitol.* **39**, 91–96 (2009).
7. Riglar, D. T. *et al.* Super-resolution dissection of coordinated events during malaria parasite invasion of the human erythrocyte. *Cell Host Microbe* **9**, 9–20 (2011).
This study uses 3D SIM imaging to visualize the invasion of human erythrocytes by *P. falciparum* merozoites, and identifies key steps in invasion, including specific tight junction formation and commitment to invasion.
8. Amino, R. *et al.* Quantitative imaging of *Plasmodium* transmission from mosquito to mammal. *Nat. Med.* **12**, 220–224 (2006).
This paper reports two previously unknown phenomena: that only a portion of the parasites that are deposited in the skin enter blood capillaries, and that many parasites are drained into the lymphatics, where they are mostly destroyed.
9. Tavares, J. *et al.* Role of host cell traversal by the malaria sporozoite during liver infection. *J. Exp. Med.* **210**, 905–915 (2013).
This investigation is the first to show that sporozoites can enter the liver hepatocytes through several pathways, including cell traversal-dependent and cell traversal-independent mechanisms.
10. Münter, S. *et al. Plasmodium* sporozoite motility is modulated by the turnover of discrete adhesion sites. *Cell Host Microbe* **6**, 551–562 (2009).
11. Gruring, C. *et al.* Development and host cell modifications of *Plasmodium falciparum* blood stages in four dimensions. *Nat. Commun.* **2**, 165 (2011).
This work uses time-lapse imaging to identify host cell modifications throughout the complete *P. falciparum* life cycle *in vitro*.
12. Prado, M. *et al.* Long-term live imaging reveals cytosolic immune responses of host hepatocytes against *Plasmodium* infection and parasite escape mechanisms. *Autophagy* **11**, 1561–1579 (2015).
13. Vanderberg, J. P., Rhodin, J. & Yoeli, M. Electron microscopic and histochemical studies of sporozoite formation in *Plasmodium berghei*. *J. Protozool.* **14**, 82–103 (1967).
14. Russell, D. G. & Sinden, R. E. Three-dimensional study of the intact cytoskeleton of coccidian sporozoites. *Int. J. Parasitol.* **12**, 221–226 (1982).
15. Dubremetz, J. F., Garcia-Réguet, N., Conseil, V. & Fourmaux, M. N. Apical organelles and host-cell invasion by Apicomplexa. *Int. J. Parasitol.* **28**, 1007–1013 (1998).
16. Kudryashev, M., Lepper, S., Baumeister, W., Cyrklaff, M. & Frischknecht, F. Geometric constrains for detecting short actin filaments by cryogenic electron tomography. *PMC Biophys.* **3**, 6 (2010).
17. Khater, E. I., Sinden, R. E. & Dessens, J. T. A malaria membrane skeletal protein is essential for normal morphogenesis, motility, and infectivity of sporozoites. *J. Cell Biol.* **167**, 425–432 (2004).
18. Battista, A., Frischknecht, F. & Schwarz, U. S. Geometrical model for malaria parasite migration in structured environments. *Phys. Rev. E Stat. Nonlin. Soft Matter Phys.* **90**, 042720 (2014).
19. Hopp, C. S. *et al.* Longitudinal analysis of *Plasmodium* sporozoite motility in the dermis reveals component of blood vessel recognition. *eLife* **4**, e07789 (2015).
20. Vanderberg, J. P. & Frevert, U. Intravital microscopy demonstrating antibody-mediated immobilisation of *Plasmodium berghei* sporozoites injected into skin by mosquitoes. *Int. J. Parasitol.* **34**, 991–996 (2004).
21. Montagna, G. N. *et al.* Critical role for heat shock protein 20 (HSP20) in migration of malarial sporozoites. *J. Biol. Chem.* **287**, 2410–2422 (2012).
22. Hellmann, J. K. *et al.* Environmental constraints guide migration of malaria parasites during transmission. *PLoS Pathog.* **7**, e1002080 (2011).
23. Formaglio, P., Tavares, J., Menard, R. & Amino, R. Loss of host cell plasma membrane integrity following cell traversal by *Plasmodium* sporozoites in the skin. *Parasitol. Int.* **63**, 237–244 (2014).
24. Amino, R. *et al.* Host cell traversal is important for progression of the malaria parasite through the dermis to the liver. *Cell Host Microbe* **3**, 88–96 (2008).
25. Menard, R. *et al.* Looking under the skin: the first steps in malarial infection and immunity. *Nat. Rev. Microbiol.* **11**, 701–712 (2013).
26. Sinnis, P. & Coppi, A. A. Long and winding road: the *Plasmodium* sporozoite's journey in the mammalian host. *Parasitol. Int.* **56**, 171–178 (2007).
27. Gueirard, P. *et al.* Development of the malaria parasite in the skin of the mammalian host. *Proc. Natl Acad. Sci. USA* **107**, 18640–18645 (2010).
28. Douglas, R. G., Amino, R., Sinnis, P. & Frischknecht, F. Active migration and passive transport of malaria parasites. *Trends Parasitol.* **31**, 357–362 (2015).
29. Panchal, D. & Bhanot, P. Activity of a trisubstituted pyrrole in inhibiting sporozoite invasion and blocking malaria infection. *Antimicrob. Agents Chemother.* **54**, 4269–4274 (2010).
30. Hellmann, J. K., Münter, S., Wink, M. & Frischknecht, F. Synergistic and additive effects of epigallocatechin gallate and digitonin on *Plasmodium* sporozoite survival and motility. *PLoS ONE* **5**, e8682 (2010).
31. Hegge, S. *et al.* Multistep adhesion of *Plasmodium* sporozoites. *FASEB J.* **24**, 2222–2234 (2010).
32. Perschman, N., Hellmann, J. K., Frischknecht, F. & Spatz, J. P. Induction of malaria parasite migration by synthetically tunable microenvironments. *Nano Lett.* **11**, 4468–4474 (2011).
33. Sultan, A. A. *et al.* TRAP is necessary for gliding motility and infectivity of *Plasmodium* sporozoites. *Cell* **90**, 511–522 (1997).
34. Carey, A. F. *et al.* Calcium dynamics of *Plasmodium berghei* sporozoite motility. *Cell. Microbiol.* **16**, 768–783 (2014).
35. Bane, K. S. *et al.* The actin filament-binding protein coronin regulates motility in *Plasmodium* sporozoites. *PLoS Pathog.* **12**, e1005710 (2016).
36. Soldati, D., Foth, B. J. & Cowman, A. F. Molecular and functional aspects of parasite invasion. *Trends Parasitol.* **20**, 567–574 (2004).
37. Hegge, S. *et al.* Direct manipulation of malaria parasites with optical tweezers reveals distinct functions of *Plasmodium* surface proteins. *ACS Nano* **6**, 4648–4662 (2012).
38. Quadt, K. A., Streichfuss, M., Moreau, C. A., Spatz, J. P. & Frischknecht, F. Coupling of retrograde flow to force production during malaria parasite migration. *ACS Nano* **10**, 2091–2102 (2016).
39. Hochstetter, A. & Pfohl, T. Motility, force generation, and energy consumption of unicellular parasites. *Trends Parasitol.* **32**, 531–541 (2016).
40. Voza, T., Miller, J. L., Kappe, S. H. & Sinnis, P. Extrahepatic exoerythrocytic forms of rodent malaria parasites at the site of inoculation: Clearance after immunization, susceptibility to primaquine, and contribution to blood-stage infection. *Infect. Immun.* **80**, 2158–2164 (2012).
41. Frevert, U., Späth, G. F. & Yee, H. Exoerythrocytic development of *Plasmodium gallinaceum* in the white leghorn chicken. *Int. J. Parasitol.* **38**, 655–672 (2008).
42. Chakravarty, S. *et al.* CD8$^+$ T lymphocytes protective against malaria liver stages are primed in skin-draining lymph nodes. *Nat. Med.* **13**, 1035–1041 (2007).
43. Coppi, A. *et al.* The malaria circumsporozoite protein has two functional domains, each with distinct roles as sporozoites journey from mosquito to mammalian host. *J. Exp. Med.* **208**, 341–356 (2011).
44. Prudencio, M., Rodriguez, A. & Mota, M. M. The silent path to thousands of merozoites: the *Plasmodium* liver stage. *Nat. Rev. Microbiol.* **4**, 849–856 (2006).
45. Sturm, A. *et al.* Manipulation of host hepatocytes by the malaria parasite for delivery into liver sinusoids. *Science* **313**, 1287–1290 (2006).
This study includes both *in vivo* and *in vitro* experiments that unravel the last unknown stage in the life cycle of *Plasmodium* spp. parasites: the transport of hepatocyte-derived merozoites into liver sinusoids within parasite-filled host cell vesicles called merosomes.
46. Frevert, U. *et al.* Intravital observation of *Plasmodium berghei* sporozoite infection of the liver. *PLoS Biol.* **3**, e192 (2005).
47. Baer, K. *et al.* Kupffer cells are obligatory for *Plasmodium yoelii* sporozoite infection of the liver. *Cell. Microbiol.* **9**, 397–412 (2007).
48. Pradel, G. & Frevert, U. Malaria sporozoites actively enter and pass through rat Kupffer cells prior to hepatocyte invasion. *Hepatology* **33**, 1154–1165 (2001).
49. Ishino, T., Chinzei, Y. & Yuda, M. A *Plasmodium* sporozoite protein with a membrane attack complex domain is required for breaching the liver sinusoidal cell layer prior to hepatocyte infection. *Cell. Microbiol.* **7**, 199–208 (2005).
50. Vestweber, D. How leukocytes cross the vascular endothelium. *Nat. Rev. Immunol.* **15**, 692–704 (2015).
51. Bano, N., Romano, J. D., Jayabalasingham, B. & Coppens, I. Cellular interactions of *Plasmodium* liver stage with its host mammalian cell. *Int. J. Parasitol.* **37**, 1329–1341 (2007).
52. Grützke, J. *et al.* The spatiotemporal dynamics and membranous features of the *Plasmodium* liver stage tubovesicular network. *Traffic* **15**, 362–382 (2014).
53. Sturm, A. *et al.* Alteration of the parasite plasma membrane and the parasitophorous vacuole membrane during exo-erythrocytic development of malaria parasites. *Protist* **160**, 51–63 (2009).
54. Ingmundson, A., Nahar, C., Brinkmann, V., Lehmann, M. J. & Matuschewski, K. The exported *Plasmodium berghei* protein IBIS1 delineates membranous structures in infected red blood cells. *Mol. Microbiol.* **83**, 1229–1243 (2012).
55. Mueller, A.-K. *et al. Plasmodium* liver stage developmental arrest by depletion of a protein at the parasite–host interface. *Proc. Natl Acad. Sci. USA* **102**, 3022–3027 (2005).
56. Mueller, A.-K., Labaied, M., Kappe, S. H. I. & Matuschewski, K. Genetically modified *Plasmodium* parasites as a protective experimental malaria vaccine. *Nature* **433**, 164–167 (2005).
57. Orito, Y. *et al.* Liver-specific protein 2: a *Plasmodium* protein exported to the hepatocyte cytoplasm and required for merozoite formation. *Mol. Microbiol.* **87**, 66–79 (2013).
58. Thieleke-Matos, C. *et al.* Host cell autophagy contributes to *Plasmodium* liver development. *Cell. Microbiol.* **18**, 437–450 (2016).
59. Gomes-Santos, C. S. S. *et al.* Highly dynamic host actin reorganization around developing *Plasmodium* inside hepatocytes. *PLoS ONE* **7**, e29408 (2012).
60. Graewe, S. *et al.* Hostile takeover by *Plasmodium*: reorganization of parasite and host cell membranes during liver stage egress. *PLoS Pathog.* **7**, e1002224 (2011).
61. Vaughan, A. M. *et al.* Complete *Plasmodium falciparum* liver-stage development in liver-chimeric mice. *J. Clin. Invest.* **122**, 3618–3628 (2012).
62. Spillman, N. J., Beck, J. R. & Goldberg, D. E. Protein export into malaria parasite-infected erythrocytes: mechanisms and functional consequences. *Annu. Rev. Biochem.* **84**, 813–841 (2015).
63. Mundwiler-Pachlatko, E. & Beck, H.-P. Maurer's clefts, the enigma of *Plasmodium falciparum*. *Proc. Natl Acad. Sci. USA* **110**, 19987–19994 (2013).
64. Wissing, F., Sanchez, C. P., Rohrbach, P., Ricken, S. & Lanzer, M. Illumination of the malaria parasite *Plasmodium falciparum* alters intracellular pH. Implications for live cell imaging. *J. Biol. Chem.* **277**, 37747–37755 (2002).

65. Haase, S. & de Koning-Ward, T. F. New insights into protein export in malaria parasites. *Cell. Microbiol.* **12**, 580–587 (2010).
66. Maier, A. G., Cooke, B. M., Cowman, A. F. & Tilley, L. Malaria parasite proteins that remodel the host erythrocyte. *Nat. Rev. Microbiol.* **7**, 341–354 (2009).
67. Spielmann, T. *et al.* A cluster of ring stage-specific genes linked to a locus implicated in cytoadherence in *Plasmodium falciparum* codes for PEXEL-negative and PEXEL-positive proteins exported into the host cell. *Mol. Biol. Cell* **17**, 3613–3624 (2006).
68. Spycher, C. *et al.* Genesis of and trafficking to the Maurer's clefts of *Plasmodium falciparum*-infected erythrocytes. *Mol. Cell. Biol.* **26**, 4074–4085 (2006).
69. Tilley, L., Sougrat, R., Lithgow, T. & Hanssen, E. The twists and turns of Maurer's cleft trafficking in *P. falciparum*-infected erythrocytes. *Traffic* **9**, 187–197 (2008).
70. de Koning-Ward, T. F., Dixon, M. W. A., Tilley, L. & Gilson, P. R. *Plasmodium* species: master renovators of their host cells. *Nat. Rev. Microbiol.* **14**, 494–507 (2016).
71. Papakrivos, J., Newbold, C. I. & Lingelbach, K. A potential novel mechanism for the insertion of a membrane protein revealed by a biochemical analysis of the *Plasmodium falciparum* cytoadherence molecule PfEMP-1. *Mol. Microbiol.* **55**, 1272–1284 (2005).
72. Taraschi, T. F., Trelka, D., Martinez, S., Schneider, T. & O'Donnell, M. E. Vesicle-mediated trafficking of parasite proteins to the host cell cytosol and erythrocyte surface membrane in *Plasmodium falciparum* infected erythrocytes. *Int. J. Parasitol.* **31**, 1381–1391 (2001).
73. Hanssen, E. *et al.* Electron tomography of the Maurer's cleft organelles of *Plasmodium falciparum*-infected erythrocytes reveals novel structural features. *Mol. Microbiol.* **67**, 703–718 (2008).
Together with reference 4, this study uses sophisticated cryoelectron and electron tomography experiments to show that Maurer's clefts are connected to the RBC membrane by stalk-like tethers and/or host-derived actin cytoskeleton, which the parasite induces and to which transport vesicles are attached.
74. Hanssen, E. *et al.* Cryo transmission X-ray imaging of the malaria parasite, *P. falciparum*. *J. Struct. Biol.* **173**, 161–168 (2011).
75. Hanssen, E. *et al.* Whole cell imaging reveals novel modular features of the exomembrane system of the malaria parasite, *Plasmodium falciparum*. *Int. J. Parasitol.* **40**, 123–134 (2010).
76. Pachlatko, E. *et al.* MAHRP2, an exported protein of *Plasmodium falciparum*, is an essential component of Maurer's cleft tethers. *Mol. Microbiol.* **77**, 1136–1152 (2010).
77. Rug, M. *et al.* Export of virulence proteins by malaria-infected erythrocytes involves remodeling of host actin cytoskeleton. *Blood* **124**, 3459–3468 (2014).
78. Bannister, L. H. & Mitchell, G. H. The malaria merozoite, forty years on. *Parasitology* **136**, 1435–1444 (2009).
79. Gilberger, T.-W., Thompson, J. K., Reed, M. B., Good, R. T. & Cowman, A. F. The cytoplasmic domain of the *Plasmodium falciparum* ligand EBA-175 is essential for invasion but not protein trafficking. *J. Cell Biol.* **162**, 317–327 (2003).
80. Rayner, J. C., Vargas-Serrato, E., Huber, C. S., Galinski, M. R. & Barnwell, J. W. A *Plasmodium falciparum* homologue of *Plasmodium vivax* reticulocyte binding protein (PvRBP1) defines a trypsin-resistant erythrocyte invasion pathway. *J. Exp. Med.* **194**, 1571–1582 (2001).
81. Singh, K. *et al.* Subdomain 3 of *Plasmodium falciparum* VAR2CSA DBL3x is identified as a minimal chondroitin sulfate A-binding region. *J. Biol. Chem.* **285**, 24855–24862 (2010).
82. Srinivasan, P. *et al.* Binding of *Plasmodium* merozoite proteins RON2 and AMA1 triggers commitment to invasion. *Proc. Natl Acad. Sci. USA* **108**, 13275–13280 (2011).
83. Weiner, A. *et al.* 3D nuclear architecture reveals coupled cell cycle dynamics of chromatin and nuclear pores in the malaria parasite *Plasmodium falciparum*. *Cell. Microbiol.* **13**, 967–977 (2011).
84. Keeley, A. & Soldati, D. The glideosome: a molecular machine powering motility and host-cell invasion by Apicomplexa. *Trends Cell Biol.* **14**, 528–532 (2004).
85. Besteiro, S., Dubremetz, J.-F. & Lebrun, M. The moving junction of apicomplexan parasites: a key structure for invasion. *Cell. Microbiol.* **13**, 797–805 (2011).
86. Lamarque, M. *et al.* The RON2–AMA1 interaction is a critical step in moving junction-dependent invasion by apicomplexan parasites. *PLoS Pathog.* **7**, e1001276 (2011).
87. Richard, D. *et al.* Interaction between *Plasmodium falciparum* apical membrane antigen 1 and the rhoptry neck protein complex defines a key step in the erythrocyte invasion process of malaria parasites. *J. Biol. Chem.* **285**, 14815–14822 (2010).
88. Giovannini, D. *et al.* Independent roles of apical membrane antigen 1 and rhoptry neck proteins during host cell invasion by Apicomplexa. *Cell Host Microbe* **10**, 591–602 (2011).
89. Lamarque, M. H. *et al.* Plasticity and redundancy among AMA–RON pairs ensure host cell entry of *Toxoplasma* parasites. *Nat. Commun.* **5**, 4098 (2014).
90. Yap, A. *et al.* Conditional expression of apical membrane antigen 1 in *Plasmodium falciparum* shows it is required for erythrocyte invasion by merozoites. *Cell. Microbiol.* **16**, 642–656 (2014).
91. Bargieri, D. Y. *et al.* Apical membrane antigen 1 mediates apicomplexan parasite attachment but is dispensable for host cell invasion. *Nat. Commun.* **4**, 2552 (2013).
92. Li, D. *et al.* Extended-resolution structured illumination imaging of endocytic and cytoskeletal dynamics. *Science* **349**, aab3500 (2015).
93. Crick, A. J. *et al.* Quantitation of malaria parasite–erythrocyte cell–cell interactions using optical tweezers. *Biophys. J.* **107**, 846–853 (2014).
94. Dasgupta, S. *et al.* Membrane-wrapping contributions to malaria parasite invasion of the human erythrocyte. *Biophys. J.* **107**, 43–54 (2014).
95. Abkarian, M., Massiera, G., Berry, L., Roques, M. & Braun-Breton, C. A novel mechanism for egress of malarial parasites from red blood cells. *Blood* **117**, 4118–4124 (2011).
96. Koussis, K. *et al.* A multifunctional serine protease primes the malaria parasite for red blood cell invasion. *EMBO J.* **28**, 725–735 (2009).
97. Joice, R. *et al. Plasmodium falciparum* transmission stages accumulate in the human bone marrow. *Sci. Transl. Med.* **6**, 244re5 (2014).
98. Dearnley, M. K. *et al.* Origin, composition, organization and function of the inner membrane complex of *Plasmodium falciparum* gametocytes. *J. Cell Sci.* **125**, 2053–2063 (2012).
99. Dearnley, M. *et al.* Reversible host cell remodeling underpins deformability changes in malaria parasite sexual blood stages. *Proc. Natl Acad. Sci. USA* **113**, 4800–4805 (2016).
100. Aingaran, M. *et al.* Host cell deformability is linked to transmission in the human malaria parasite *Plasmodium falciparum*. *Cell. Microbiol.* **14**, 983–993 (2012).
This research quantitatively assesses the changes in gametocyte deformability at different stages of maturation, using *in vitro* capillary assays and 3D finite-element whole-cell modelling.
101. Chotivanich, K. *et al.* Central role of the spleen in malaria parasite clearance. *J. Infect. Dis.* **185**, 1538–1541 (2002).
102. del Portillo, H. A. *et al.* The role of the spleen in malaria. *Cell. Microbiol.* **14**, 343–355 (2012).
103. Engwerda, C. R., Beattie, L. & Amante, F. H. The importance of the spleen in malaria. *Trends Parasitol.* **21**, 75–80 (2005).
104. Buffet, P. A. *et al.* The pathogenesis of *Plasmodium falciparum* malaria in humans: insights from splenic physiology. *Blood* **117**, 381–392 (2011).
105. Hanssen, E. *et al.* Soft X-ray microscopy analysis of cell volume and hemoglobin content in erythrocytes infected with asexual and sexual stages of *Plasmodium falciparum*. *J. Struct. Biol.* **177**, 224–232 (2012).
106. Kono, M. *et al.* Evolution and architecture of the inner membrane complex in asexual and sexual stages of the malaria parasite. *Mol. Biol. Evol.* **29**, 2113–2132 (2012).
107. Hliscs, M. *et al.* Organization and function of an actin cytoskeleton in *Plasmodium falciparum* gametocytes. *Cell. Microbiol.* **17**, 207–225 (2015).
108. Schröder, R. R. Advances in electron microscopy: a qualitative view of instrumentation development for macromolecular imaging and tomography. *Arch. Biochem. Biophys.* **581**, 25–38 (2015).
109. Mahamid, J. *et al.* Visualizing the molecular sociology at the HeLa cell nuclear periphery. *Science.* **351**, 969–972 (2016).
110. Zhang, P. Correlative cryo-electron tomography and optical microscopy of cells. *Curr. Opin. Struct. Biol.* **23**, 763–770 (2013).
111. Pampaloni, F., Ansari, N. & Stelzer, E. H. High-resolution deep imaging of live cellular spheroids with light-sheet-based fluorescence microscopy. *Cell Tissue Res.* **352**, 161–177 (2013).
112. Lemon, W. C. *et al.* Whole-central nervous system functional imaging in larval *Drosophila*. *Nat. Commun.* **6**, 7924 (2015).
113. Tomer, R., Khairy, K., Amat, F. & Keller, P. J. Quantitative high-speed imaging of entire developing embryos with simultaneous multiview light-sheet microscopy. *Nat. Methods* **9**, 755–763 (2012).
114. Wilson, L. G., Carter, L. M. & Reece, S. E. High-speed holographic microscopy of malaria parasites reveals ambidextrous flagellar waveforms. *Proc. Natl Acad. Sci. USA* **110**, 18769–18774 (2013).
This report explores a novel imaging technique (high-speed holographic microscopy) to reveal the relevance of chirality in the structure of the axoneme and microtubules in male gametes: their chirality is linked with the beating motion of the gamete.
115. Martin, K. *et al.* Spatio-temporal co-ordination of RhoA, Rac1 and Cdc42 activation during prototypical edge protrusion and retraction dynamics. *Sci. Rep.* **6**, 21901 (2016).
116. Cohen, A. E. Optogenetics: turning the microscope on its head. *Biophys. J.* **110**, 997–1003 (2016).
117. Chen, B.-C. *et al.* Lattice light sheet microscopy: imaging molecules to embryos at high spatiotemporal resolution. *Science* **346**, 1257998 (2014).
118. Nikič, I. *et al.* Minimal tags for rapid dual-color live-cell labeling and super-resolution microscopy. *Angew. Chem. Int. Ed. Engl.* **53**, 2245–2249 (2014).
119. Lemke, E. A. & Schultz, C. Principles for designing fluorescent sensors and reporters. *Nat. Chem. Biol.* **7**, 480–483 (2011).
120. Li, A. *et al.* Molecular mechanistic insights into the endothelial receptor mediated cytoadherence of *Plasmodium falciparum*-infected erythrocytes. *PLoS ONE* **6**, e16929 (2011).
121. Li, A., Mansoor, A. H., Tan, K. S. W. & Lim, C. T. Observations on the internal and surface morphology of malaria infected blood cells using optical and atomic force microscopy. *J. Microbiol. Methods* **66**, 434–439 (2006).
122. Quadt, K. A. *et al.* The density of knobs on *Plasmodium falciparum*-infected erythrocytes depends on developmental age and varies among isolates. *PLoS ONE* **7**, e45658 (2012).
123. Aikawa, M. *et al.* Membrane knobs of unfixed *Plasmodium falciparum*-infected erythrocytes: new findings as revealed by atomic force microscopy and surface potential spectroscopy. *Exp. Parasitol.* **84**, 339–343 (1996).
124. Carvalho, P. A., Diez–Silva, M., Chen, H., Dao, M. & Suresh, S. Cytoadherence of erythrocytes invaded by *Plasmodium falciparum*: quantitative contact-probing of a human malaria receptor. *Acta Biomater.* **9**, 6349–6359 (2013).
125. Xu, X. *et al.* Probing the cytoadherence of malaria infected red blood cells under flow. *PLoS ONE* **8**, e64763 (2013).
126. Ando, T., Uchihashi, T. & Kodera, N. High-speed AFM and applications to biomolecular systems. *Annu. Rev. Biophys.* **42**, 393–414 (2013).
127. Shibata, M., Uchihashi, T., Ando, T. & Yasuda, R. Long-tip high-speed atomic force microscopy for nanometer-scale imaging in live cells. *Sci. Rep.* **5**, 8724 (2015).
128. Müller, D. J. & Dufrêne, Y. F. Atomic force microscopy as a multifunctional molecular toolbox in nanobiotechnology. *Nat. Nanotechnol.* **3**, 261–269 (2008).
129. Regev-Rudzki, N. *et al.* Cell–cell communication between malaria-infected red blood cells via exosome-like vesicles. *Cell* **153**, 1120–1133 (2013).
130. Mantel, P.-Y. *et al.* Malaria infected erythrocyte-derived microvesicles mediate cellular communication within the parasite population and with the host immune system. *Cell Host Microbe* **13**, 521–534 (2013).
Together with reference 129, this report presents the finding that RBCs infected with *P. falciparum* use microvesicles and exosomes to stimulate the production of transmission stages, and that these vesicles have immunomodulatory properties.
131. Martin-Jaular, L., Nakayasu, E. S., Ferrer, M., Almeida, I. C. & del Portillo, H. A. Exosomes from *Plasmodium yoelii*-infected reticulocytes protect mice from lethal infections. *PLoS ONE* **6**, e26588 (2011).
132. Rongvaux, A. *et al.* Human hemato-lymphoid system mice: current use and future potential for medicine. *Annu. Rev. Immunol.* **31**, 635–674 (2013).

133. Vaughan, A. M., Kappe, S. H. I., Ploss, A. & Mikolajczak, S. A. Development of humanized mouse models to study human malaria parasite infection. *Future Microbiol.* **7**, 657–665 (2012).
134. Soulard, V. *et al. Plasmodium falciparum* full life cycle and *Plasmodium ovale* liver stages in humanized mice. *Nat. Commun.* **6**, 7690 (2015).
135. Mikolajczak, S. A. *et al. Plasmodium vivax* liver stage development and hypnozoite persistence in human liver-chimeric mice. *Cell Host Microbe* **17**, 526–535 (2015).
136. Mota, M. M. *et al.* Migration of *Plasmodium* sporozoites through cells before infection. *Science.* **291**, 141–144 (2001).
This study demostrates that sporozoites traverse several cells prior to switching from a traversal to an invasion mode in a final hepatocyte, in which they will fully develop.
137. Nacer, A. *et al.* Experimental cerebral malaria pathogenesis — hemodynamics at the blood brain barrier. *PLoS Pathog.* **10**, e1004528 (2014).
This exhaustive investigation uses IVM to elucidate the role of several leukocytes in the brain, finding that during cerebral malaria, a severe restriction in venous blood flow efflux from the brain results in oedema and, ultimately, cranial hypertension.
138. Kudryashev, M. *et al.* Positioning of large organelles by a membrane-associated cytoskeleton in *Plasmodium* sporozoites. *Cell. Microbiol.* **12**, 362–371 (2010).
139. McMillan, P. J. *et al.* Spatial and temporal mapping of the PfEMP1 export pathway in *Plasmodium falciparum*. *Cell. Microbiol.* **15**, 1401–1418 (2013).
140. Eaton, P., Zuzarte-Luis, V., Mota, M. M., Santos, N. C. & Prudêncio, M. Infection by *Plasmodium* changes shape and stiffness of hepatic cells. *Nanomedicine* **8**, 17–19 (2012).
141. Lučič, V., Rigort, A. & Baumeister, W. Cryo-electron tomography: the challenge of doing structural biology *in situ*. *J. Cell Biol.* **202**, 407–419 (2013).
142. Oikonomou, C. M. & Jensen, G. J. A new view into prokaryotic cell biology from electron cryotomography. *Nat. Rev. Microbiol.* **14**, 205–220 (2016).
143. Hanssen, E. *et al.* Electron tomography of *Plasmodium falciparum* merozoites reveals core cellular events that underpin erythrocyte invasion. *Cell. Microbiol.* **15**, 1457–1472 (2013).
144. Nans, A., Mohandas, N. & Stokes, D. L. Native ultrastructure of the red cell cytoskeleton by cryo-electron tomography. *Biophys. J.* **101**, 2341–2350 (2011).
145. Carzaniga, R., Domart, M.-C., Collinson, L. M. & Duke, E. Cryo-soft X-ray tomography: a journey into the world of the native-state cell. *Protoplasma* **251**, 449–458 (2014).
146. Shroff, H., Galbraith, C. G., Galbraith, J. A. & Betzig, E. Live-cell photoactivated localization microscopy of nanoscale adhesion dynamics. *Nat. Methods* **5**, 417–423 (2008).
147. Hell, S. W. Toward fluorescence nanoscopy. *Nat. Biotechnol.* **21**, 1347–1355 (2003).
148. Folling, J. *et al.* Fluorescence nanoscopy by ground-state depletion and single-molecule return. *Nat. Methods* **5**, 943–945 (2008).
149. Absalon, S., Robbins, J. A. & Dvorin, J. D. An essential malaria protein defines the architecture of blood-stage and transmission-stage parasites. *Nat. Commun.* **7**, 11449 (2016).
150. Nakano, A. Spinning-disk confocal microscopy; a cutting-edge tool for imaging of membrane traffic. *Cell Struct. Funct.* **27**, 349–355 (2002).
151. Svoboda, K. & Yasuda, R. Principles of two-photon excitation microscopy and its applications to neuroscience. *Neuron* **50**, 823–839 (2006).
152. Bush, P. G., Wokosin, D. L. & Hall, A. C. Two-versus one photon excitation laser scanning microscopy: critical importance of excitation wavelength. *Front. Biosci.* **12**, 2646–2657 (2007).
153. Chen, X., Nadiarynkh, O., Plotnikov, S. & Campagnola, P. J. Second harmonic generation microscopy for quantitative analysis of collagen fibrillar structure. *Nat. Protoc.* **7**, 654–669 (2012).
154. Oron, D. *et al.* Depth-resolved structural imaging by third-harmonic generation microscopy. *J. Struct. Biol.* **147**, 3–11 (2004).
155. Paddock, S. W. Principles and practices of laser scanning confocal microscopy. *Mol. Biotechnol.* **16**, 127–149 (2000).
156. Kehrer, J. *et al.* R., A putative small solute transporter is responsible for the secretion of G377 and TRAP-containing secretory vesicles during *Plasmodium* gamete egress and sporozoite motility. *PLoS Pathog.* **12**, e1005734 (2016).
157. Matz, J. M. *et al.* The *Plasmodium berghei* translocon of exported proteins reveals spatiotemporal dynamics of tubular extensions. *Sci. Rep.* **5**, 12532 (2015).
158. Neuman, K. C. & Nagy, A. Single-molecule force spectroscopy: optical tweezers, magnetic tweezers and atomic force microscopy. *Nat. Methods* **5**, 491–505 (2008).
159. Masedunskas, A. *et al.* Intravital microscopy: a practical guide on imaging intracellular structures in live animals. *Bioarchitecture* **2**, 143–157 (2012).
160. Pittet, M. J. & Weissleder, R. Intravital imaging. *Cell* **147**, 983–991 (2011).
161. de Moraes, L. V., Tadokoro, C. E., Gomez-Conde, I., Olivieri, D. N. & Penha-Gonçalves, C. Intravital placenta imaging reveals microcirculatory dynamics impact on sequestration and phagocytosis of *Plasmodium*-infected erythrocytes. *PLoS Pathog.* **9**, e1003154 (2013).
162. Radtke, A. J. *et al.* Lymph-node resident CD8α$^+$ dendritic cells capture antigens from migratory malaria sporozoites and induce CD8$^+$ T cell responses. *PLoS Pathog.* **11**, e1004637 (2015).
163. Lawton, J. C., Benson, R. A., Garside, P. & Brewer, J. M. Using lymph node transplantation as an approach to image cellular interactions between the skin and draining lymph nodes during parasitic infections. *Parasitol. Int.* **63**, 165–170 (2014).
164. Ferrer, M., Martin-Jaular, L., Calvo, M. & del Portillo, H. A. Intravital microscopy of the spleen: quantitative analysis of parasite mobility and blood flow. *J. Vis. Exp.* http://dx.doi.org/10.3791/3609 (2012).
165. De Niz, M. *et al.* The machinery underlying malaria parasite virulence is conserved between rodent and human malaria parasites. *Nat. Commun.* **7**, 11659 (2016).

Acknowledgements
The authors are grateful to J. Brewer, U. Frevert, M. Marti, C. Agop-Nersesian, R. Douglas, C. Grüring and B. Zuber for helpful comments and suggestions, and N. Brancucci for help with figure 4d. They also thank the Microscope Imaging Center (MIC) at the University of Bern, Switzerland, for outstanding technical support. M.D.N., H.A.P. and V.T.H. acknowledge funding from the European Union's Seventh Framework Program (grant 242095: EVIMalaR). T.S. acknowledges support from the research training group GRK1459 and the German Research Foundation (DFG) (grant SP1209/1). F.F. acknowledges support from the CellNetwork research cluster of Heidelberg University, Germany. Work in the F.F. laboratory is currently funded by grants from the DFG (SFB1129, FR 2140/6-1), the Human Frontier Science Program and the European Research Council. V.T.H. acknowledges support from the Swiss National Science Foundation (SNSF) (grant 310030–159519) and from SystemsX (grant 51RTPO_151032).

Competing interests statement
The authors declare no competing interests.

SUPPLEMENTARY INFORMATION
See online article: S1 (movie) | S2 (movie) | S3 (movie | S4 (movie) | S5 (movie) | S6 (movie) | S7 (movie) | S8 (movie)

ALL LINKS ARE ACTIVE IN THE ONLINE PDF